

(R)

NBSIR 78-1560

EA-77-A-01-6010 - 13
Distribution Category UC-90g

DEVELOPMENT, TESTING AND EVALUATION OF MHD-MATERIALS

Quarterly Report
for the period July - September 1978

W. R. Hosler, T. Negas and S. J. Schneider

Ceramics, Glass and Solid State Science Division
Center for Materials Science

National Bureau of Standards
Washington, D.C. 20234

Date Published: September 30, 1978

**PREPARED FOR THE UNITED STATES
DEPARTMENT OF ENERGY**

Under Contract No. EA-77-A-01-6010

"This report was prepared as an account of work sponsored by the United States Government. Neither the United States nor the United States Department of Energy, nor any of their employees, nor any of their contractors, subcontractors, or their employees, make any warranty, express or implied, or assumes any legal liability or responsibility for the accuracy, completeness, or usefulness of any information, apparatus, product or process disclosed, or represents that its use would not infringe private owned rights."

TABLE OF CONTENTS

PAGE

ABSTRACT.	1
OBJECTIVES AND SCOPE OF WORK.	2
SUMMARY OF ACHIEVEMENTS	3
TALKS AND PUBLICATIONS.	5
SUMMARY OF PROGRESS LISTED BY TASKS	
TASK G. PROGRAM MANAGEMENT AND COORDINATION.	6
TASK I. OPERATIONAL DESIGN PROPERTIES.	7
1. Viscosity of Coal Slags.	7
2. Electrical Conductivity.	12
3. Vaporization Studies	26
TASK J. CORROSION AND DIFFUSION.	29
1. Diffusion in Insulator Electrode Couples	29
2. High Temperature Charge Transport in Coal Slags.	32
3. Electrochemical Effects in Simulated Slag Flow	33
4. Seed/Slag Interactions and Slag Corrosion.	34
TASK K. MATERIALS TESTING AND CHARACTERIZATION	50
1. Structural Analysis of Powdered and Solid Ceramics	50
2. Electrode Systems and Component Materials Testing.	55
3. Test Analysis (Pre and Post Test Materials Characterization.	56
4. Materials Development and Analysis	64
TASK L. ASSESSMENT OF STEAM PLANT COMPONENTS	67
1. Laboratory Hot Corrosion Screening Program	67
2. Material Assessment.	68
TASK M. INFORMATION AND DATA ON MATERIALS FOR MHD POWER SYSTEMS.	72
1. Data Center for Materials Properties and Performance	72

NBS involvement in MHD related program review and coordination has continued.

A study was completed showing consistent increases in viscosity of several slags due to seeding with K_2O . The maximum increase was observed at 15 to 20 wt % K_2O . At 30% the viscosity was only slightly higher than unseeded slags.

A FluidDyne Corporation heater matrix effluent of seed-slag mixture (very high seed to slag ratio) was shown to be extremely fluid and to exhibit slight immiscibility.

The electrical conductivity of a number of potential MHD electrode materials has been measured.

At 2000 K the pressure of Fe(g) over MAFF-31 is about 10^{-5} atm which is about 10 times the Mg pressure. The upper temperature limit is 1600 °C.

Interdiffusion of iron between MgO insulator material and MAFF-31 ($3MgAl_2O_4:Fe_3O_4$) was measured at 1400 °C. The results indicate a strong temperature dependence, since diffusion coefficients at 1400 °C were smaller by a factor 4 to 7 than those measured previously at 1600 °C.

Initial measurements on charge transport in slag indicate that the ionic conductivity in an "Eastern" coal slag is much less than the electronic conductivity at temperatures not much higher than the softening point of the slag.

The phase compositions of six component "Eastern" and "Western" synthetic coal slags has been measured and analyzed.

Approximately 50 materials have been analyzed structurally by X-ray diffraction methods including some of those tested in the U-02 Phase III experiment.

A brief analysis of the electrodes from the recent 250 hour AVCO test is presented. Electrochemical effects apparently played a large role in the observed electrode changes but the tested electrodes were in exceptionally good conditions considering the rigors imposed by the AVCO test facility.

Several samples from a unique deposit on the E wall - B wall joint in the USSR-U-25 RM channel have been analyzed and found to contain unaltered Al_2O_3 and $AlPO_4$ on the plasma side with some β -alumina at the center and near the wall side.

Electrical conductivity measurements on a flowing layer of material joining the electrode and insulator wall of the Phase III U-02 experiment have been made. They do not prove conclusively that the steady deterioration of the interelectrode insulation during the experiment was a result of this layer which contained an inordinate amount of Al_2O_3 . The origin of the Al_2O_3 remains unexplained.

The procedures for laboratory testing of the hot corrosion of boiler tube and other steam plant components have been established. Initial tests on several materials are in progress.

Review and cataloging of contractors reports remain a continuing activity. A data base structure has been designed and loaded into a computer for test purposes. A proposal for bids from vendors of Data Base Management Systems has been submitted for Department of Commerce approval.

OBJECTIVES AND SCOPE OF WORK

The overall objective of this program is to obtain chemical and physical definition of high temperature materials which have shown promise for use in coal-fired open-cycle MHD power systems. Major problem areas in which investigations will be concentrated are:

1. Characterization of coal slag and its effects on system components and performance at prototype temperatures.
2. Development of electrode materials which provide adequate performance over extended periods of time.
3. Insulating materials which limit thermal losses and are resistant to prolonged thermal and erosion effects.
4. Preheater materials which can withstand the operating modes of separately and directly fired operation.
5. Seed recovery methods from slag which are technically and economically feasible.
6. Phase equilibria and diffusion rates of seed in slag and corrosive action of combination on system components and materials.
7. Durability of prototype MHD sub-systems.

The program is designed to contribute to the solution of these problems by providing much needed data on candidate materials and by evaluating test samples and structure that have been subjected to real or simulated MHD conditions. The activities are grouped under six tasks:

- G. Program Management Coordination (Assisting DoE in coordination, planning and review of the various MHD-Materials Development Programs).
- I. Operational Design Properties (viscosity, electrical conductivity, vaporization).
- J. Corrosion by Seed and Slag (phase equilibria, diffusion).
- K. Materials Testing and Characterization (test coordination, pre- and post-test analysis).
- L. Assessment of Steam Plant Components (corrosion resistance of metals and alloys).
- M. Information and Data on Materials for MHD Power Systems.

SUMMARY OF ACHIEVEMENTS (July-Sept. 1978)
(Completed or Continuing Milestones-See Work Plan FY 1978)

TASK G.

2. Participates in reviews, planning sessions, preparation of working documents in the area of MHD development (continuing).

TASK I.

6. The final series of viscosity measurements was completed which reveals the effect of K_2O seeding on the viscosity of several different coal slags (completed August 31, 1978).

9. Measure the electrical conductivity of established as well as promising (new) electrode materials (continuing).

14. Determine FeO losses over several spinel compositions which are promising electrode materials (completed September 15, 1978).

17. Determine thermochemistry in a number of critical multicomponent systems to assess slag/seed interaction, provide potassium activity data (in conjunction with vapor pressure measurements) and to define reactions leading to corrosion of construction materials (continuing).

e. Determine melting relations for the $CaSiO_3$ - $KAlSi_2O_6$ - $CaAl_2Si_2O_8$ system (pertinent to western coal ashes) (completed Sept. 15, 1978).

TASK J.

18. Determine chemical reaction processes of construction material (e.g., $LaCrO_3$ zirconia-based, etc.) with seed/slag (continuing).

23. Conduct diffusion studies in slag-insulator (spinel, MgO , Al_2O_3) systems to study penetration of Fe, Si, Ca, etc. into the insulator materials (continuing).

TASK K.

26. Coordinate testing and pre- and post-test analysis of specimens exposed to simulated or real MHD conditions in a variety of test rigs, arc heaters, small- and large-scale MHD-generators, etc. Stimulate, expedite and organize materials procurement, electrode design and preparation, test scheduling, materials evaluation, etc. Encourage and promote collaborative efforts aimed at gathering maximum information on MHD-materials and components in the minimum amount of time (continuing).

27. Use a variety of chemical and physical techniques to assess the stability (or degradation) of materials and structures tested for specific time periods of real or simulated MHD-facilities. Pre- and post-characterization of tested samples from experiments performed in the MIT test rig, AVCO and U-02 generators, etc. (continuing).

28. A system of efficient communication between MHD-workers at various institutions concerning MHD-materials and testing will be extended and formalized. This includes also the establishment of a data base management system which will be available to designers, facility operators and materials experts in the field of MHD power development (continuing).

TASK L.

31. Design and construct apparatus to provide screening of metals for corrosion-resistance to potassium and/or slag attack for MHD boiler tube applications (completed August 1, 1978).

32. Complete initial test measurements on 4-6 different materials using the above corrosion apparatus (completed September 15, 1978).

Talks and Publications

Vapor Pressure Measurements of Potassium over K_2O-SiO_2 Solutions by a Knudsen Effusion, Mass Spectrometric Method

E. R. Plante

10th Materials Research Symposium, NBS, Gaithersburg, MD
September 18-22, 1978.

Joint NBS-UTSI Cooperative Program Review

S. J. Schneider, T. Negas, J. Smith, L. P. Cook, E. N. Farabaugh, H. M. Ondik, A. Perloff from NBS and J. B. Dicks, S. Strom, J. Lanier, S. Wu, M. Beaton, N. Egan, W. Long from UTSI at the University of Tennessee Space Institute, Tullahoma, TN, July 18, 1978.

TASK G. PROGRAM MANAGEMENT AND COORDINATION (S. J. Schneider)

S. J. Schneider and other NBS staff participated in assorted DoE arranged or sanctioned program review/coordination meetings, briefings, and technical conferences. These included:

1. U.S.-U.S.S.R. Cooperative Program on MHD; Steering Committee Meeting June 18-23, 1978 (in Moscow).
2. U.S.-U.S.S.R. Steering Committee (U.S. side) planning session August 31, 1978 (in Washington).
3. Materials Meeting for Cooperative Program (U.S.-U.S.S.R.), August 23, 1978 (in Chicago).
4. UTSI visit and planning session on cooperative NBS-UTSI work, July 18, 1978 (in Tullahoma) and September 13, 1978 (at NBS).

The conclusions and recommendations resulting from these meetings and other DoE assigned activities are reflected in reports to DoE, through direct consultation with DoE staff or through documents published elsewhere.

In addition to the above, NBS is joint sponsor with DoE-Fossil Energy and others of the 3rd Annual Meeting on "Materials for Coal Conversion and Utilization", October 10-12, 1978. S. J. Schneider (NBS) and Wate Bakker, DoE, have organized the meeting; a session is devoted to MHD.

Task I. OPERATIONAL DESIGN PROPERTIES

1. Viscosity of Coal Slags (W. Capps and D. A. Kauffman)

1.1 Introduction

The principal thrust of this part of this task for several years has been an effort to find a means of predicting the viscosity of slags formed from the combustion of coal in the open cycle MHD process.

One approach has been to make a series of five component slags by melting mixtures of oxides and carbonates in the laboratory and measuring the viscosity of the resulting liquids at temperatures ranging from about 1620 to about 1200 C. Systematic changes were made to a base or starting composition by adding or subtracting one oxide at a time in 5% increments. These melts contained only the five major constituents of real coal slags; these are oxides of silicon, aluminum, iron, calcium, and magnesium.

A summary of the data for this series was presented in the report for the period ending in June 1978, in Figures 1 and 2. Figure 1 showed the data obtained at 1600 and Figure 2 the data for 1300 C. Figure 2 contains an error of omission. The curve for Al_2O_3 was left out of this figure even though the label for it was present. The corrected figure appears in this present report as Fig. 1.

1.2 Slag Preparation and Measurement

a. Seeded Series

As an extension of the previously reported series of artificial slags, K_2O is being added in order to simulate seeded-slag behavior.

K_2O was added in 5% increments up to and including 30% by weight to the slag, K-884, which is the base or starting point for the entire series. This base composition was chosen to fall between the two coal slags selected by most MHD contractors for study. They are slags from Montana Rosebud Seam coal and Illinois #6 coal. The composition of this base slag is shown in Fig. 2, which also shows the viscosity data at 1600, 1500, 1400 and 1300 C for the K_2O -base slag series.

The above series shows the same trends as those shown by several earlier series where K_2O was added to different slags. All of these indicate that K_2O causes the viscosity to increase at all concentrations up to and including 25 weight percent K_2O . Only the low silica series starting with K-488 shows a lower viscosity than the base slag due to K_2O at a concentration of 30%. These studies show that the increase reaches a maximum at 15 to 20% K_2O and that the effect of the K_2O is greater in magnitude for the low silica, low viscosity series than for the high silica, high viscosity series. Figure 3 shows this effect for several K_2O slag series, all at 1600 C.

b. Seed-Slag Heater Effluent

Viscosity was measured of a seed-slag mixture which was the effluent from the Fluidyne MHD heater matrix. The starting materials were K_2SO_4 which was injected at the rate of 19 pounds per hour and coal which was injected at the rate of 10 pounds per hour.

The viscosity was so low that it was below the recommended limit for the viscometer, but a rough figure would be 0.16 poises or $-0.8 \log_{10}$ poises. This means that this material is many times more fluid than unseeded slag.

Care was taken to observe any immiscibility or separation of seed and slag while in the liquid state. Some immiscibility was in fact observed but the heavy darker layer was present in such a small amount that its viscosity could not be measured at all. A rough estimate is that the lower layer was less than 0.1% of the total mass of the mixture.

1.3 Future Plans

In order to more closely simulate natural coal slags small amounts of the usual minor constituents will be added to the base slag to indicate the extent of their influence on viscosity. These additions will include oxides of phosphorous, titanium, sodium, and sulphur.

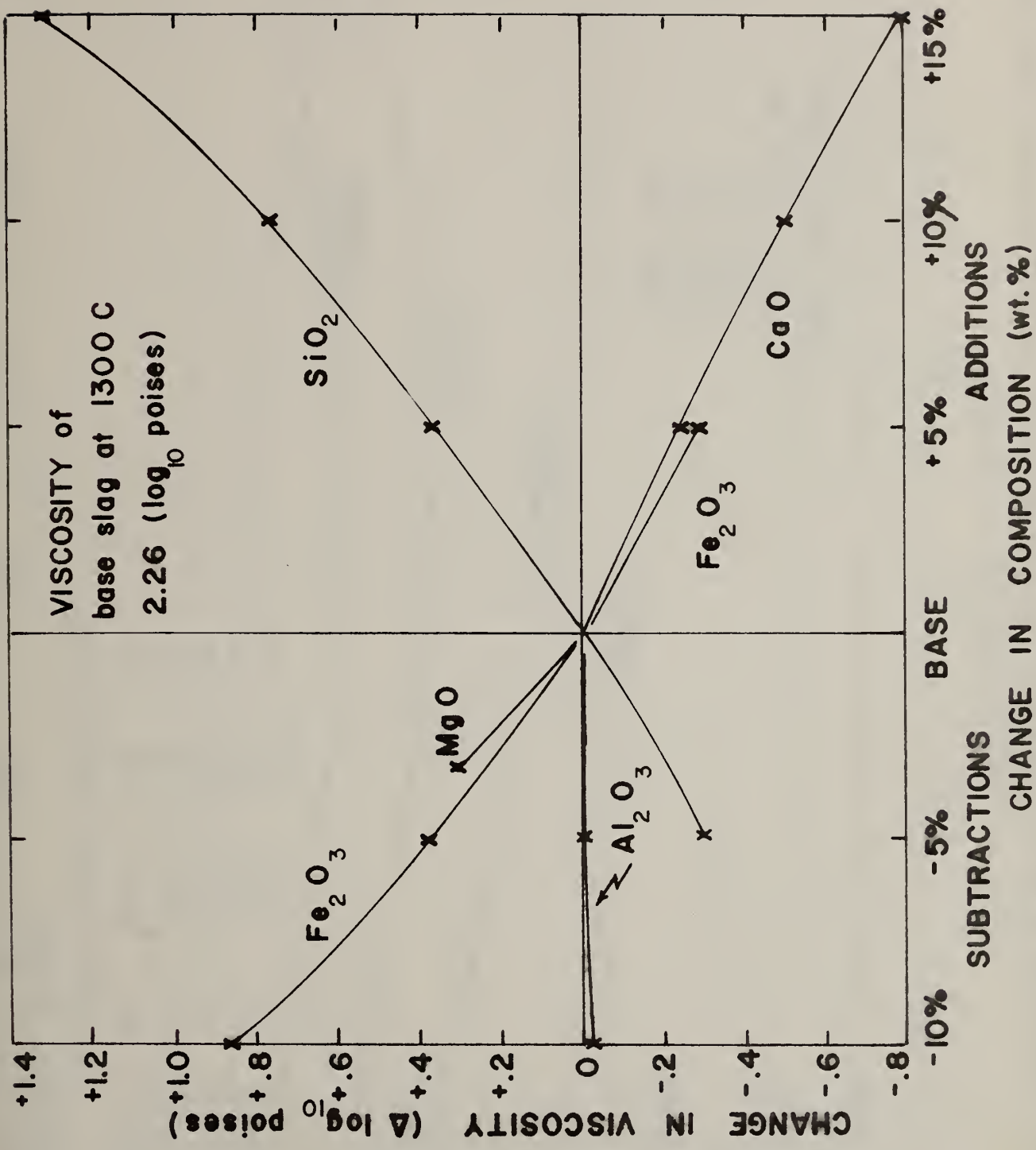
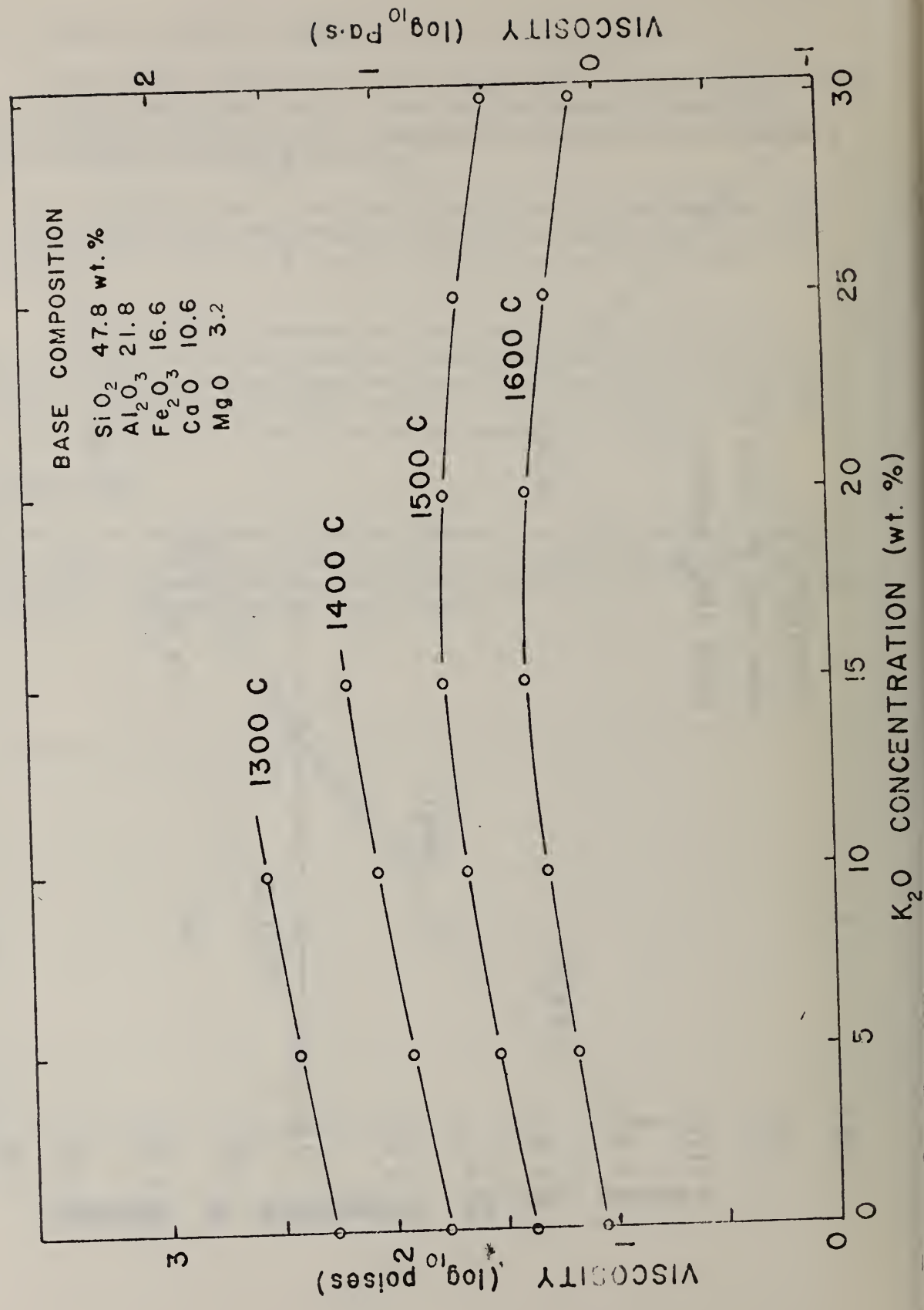


Fig. 1. The Effect of Change of Concentration of Each Oxide on the Viscosity of Base Slag K-884 at 1300 C. (47.8% SiO_2 , 21.8% Al_2O_3 , 16.6% Fe_2O_3 , 10.6% CaO, 3.3% MgO)



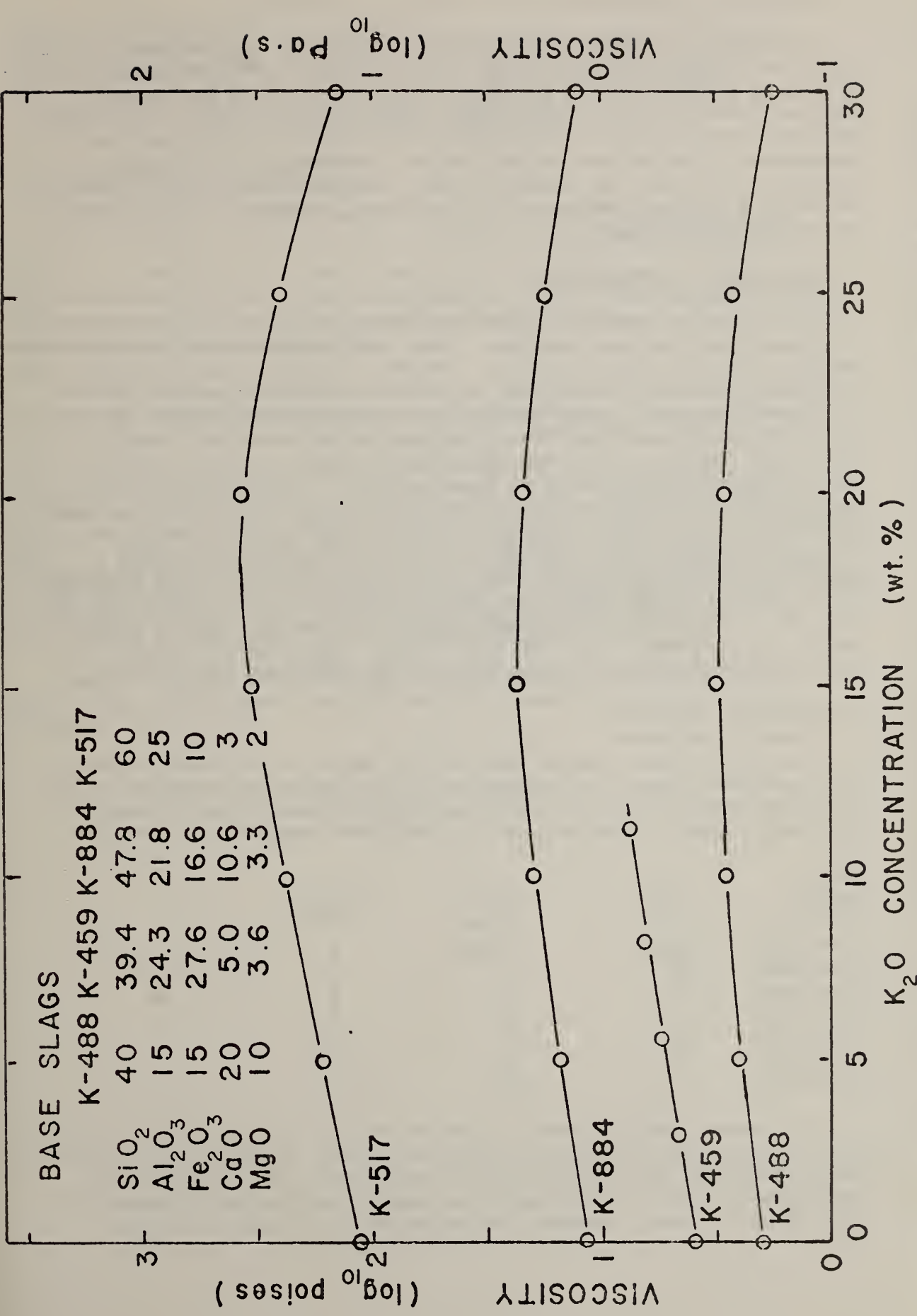


Fig. 3. The Effect of K₂O Seed Concentration on the Viscosity of Several Different Slags at 1600 C.

2. Electrical Conductivity (W. R. Hosler, J. Langley)

During this reporting period work has continued on measurement of the electrical conductivity of promising electrode materials developed at NBS or sent to us by other MHD contractors. The electrical measurements reported in this section are all made using the well known DC four probe technique thus basically eliminating difficulties due to contact emf's or resistances. The current is supplied by a constant current supply of variable voltage and the potential drop is measured across the conductivity probes by a DC electrometer with a high input impedance ($>10^{14}\Omega$) compared to the sample resistance.

2.1 U-02 Phase III Materials

The electrical conductivity of most materials used in the Phase III U-02 experiment has been measured. This data is reported in the Quarterly Report (April-June 1978, page 12). However, two additional materials used in Group 2 of the test were sent to us by Westinghouse Research and Development Center. These materials were used in place of some Group 2 Materials due to some last minute fabrication difficulties. They are from a two component electrode containing mixtures of LaCrO_3 - LaAlO_3 . The electrical data is shown in Figures 4 and 5. The conductivity of both compositions appears to be oxygen pressure dependent with the higher conductivity associated with that material containing less LaAlO_3 as expected. However, even this material in an air atmosphere would experience some joule heating when used as a leadout near room temperature. In the Phase III experiment they were attached to a nickel mesh and thus designed to have the lowest temperature well above that of the copper cooling block, however, at the cathode where oxygen pressure may be low, the electrode function could be impaired by inadequate conductivity.

2.2 MgO-Cr₂O₃ Mixtures

A series of seven samples were sent to us by Westinghouse Research and Development Center for evaluation of the electrical conductivity and phase composition. Table 1 lists the nominal compositions of these materials. Chemical analysis of the fabricated samples is in progress.

Table 1.

<u>Sample</u>	<u>MgO</u>	<u>Cr₂O₃</u>	<u>Figure</u>
MC-AT-0501	60m/o	40m/o	6
MC-AT-0601	56	44	7
MC-AT-0401	52	48	8
MC-AT-0101	50	50	9
MC-AT-0301	48	52	10
MC-AT-0701	2	98	11
CO-AT-0101	0	100	12

All these materials were hot pressed at 3000 psi and 1650 °C except for the Cr_2O_3 sample CO-AT-0101 which was pressed at 3000 psi and 1450 °C. One would expect the conductivity of the material just off the 50-50 composition on the Mg rich side to be higher than the 50-50 composition. This is not the case; however, the 56 MgO-44 Cr_2O_3 mixture has the

highest conductivity of all compositions measured. X-ray diffraction data, Task K, Section 1, page 52 of this report indicates that all materials except the Cr_2O_3 and MC-AT-0101 and MC-AT-0401 contain second phases. The pure stoichiometric material 50 MgO-50 Cr_2O_3 or MgCr_2O_4 should have a high electrical resistivity.

2.3 YCrO_3 Doped with Ca and Mg

In addition to the above series of seven samples, Westinghouse R&D has sent a sample of $\text{YMg}_{.05}\text{Cr}_{.95}\text{O}_3$ which was hot pressed at 3000 psi and 1650 °C (YC-AT-0101). The conductivity data is shown in Figure 13. This sample was very dense and there appears to be little oxygen pressure dependence except above 1600 °C. In this sample the magnesium is substituted on the chromium site.

NBS has fabricated several samples of YCrO_3 doped with calcium where the calcium has been substituted on the yttrium₃ site. These samples $\text{Y}_{.98}\text{Ca}_{.02}\text{CrO}_3$ (TT-MS-8416) and $\text{Y}_{.95}\text{Ca}_{.05}\text{CrO}_3$ (TT-MS-8417) were thermally sintered at 1746 °C for 6 hours in an atmosphere of forming gas. The former was 90.2% dense while the latter was 95.2%. Theoretical density was taken as 5.75 g/cm³. Data is shown in Figures 14 and 15. Both samples indicate a good electrical conductivity. One advantage of YCrO_3 over LaCrO_3 is the possibility of avoiding the hydration problem particularly in post test conditions when excess lanthana caused by evaporation of chromium, at high temperatures in an MHD duct, goes to lanthanum hydroxide resulting in a crumbling of the electrode material after a test.

Samples of this material doped with Ca and Mg substituted on both the yttrium and chromium sites are being hot pressed at the University of Dayton, Dayton, OH.

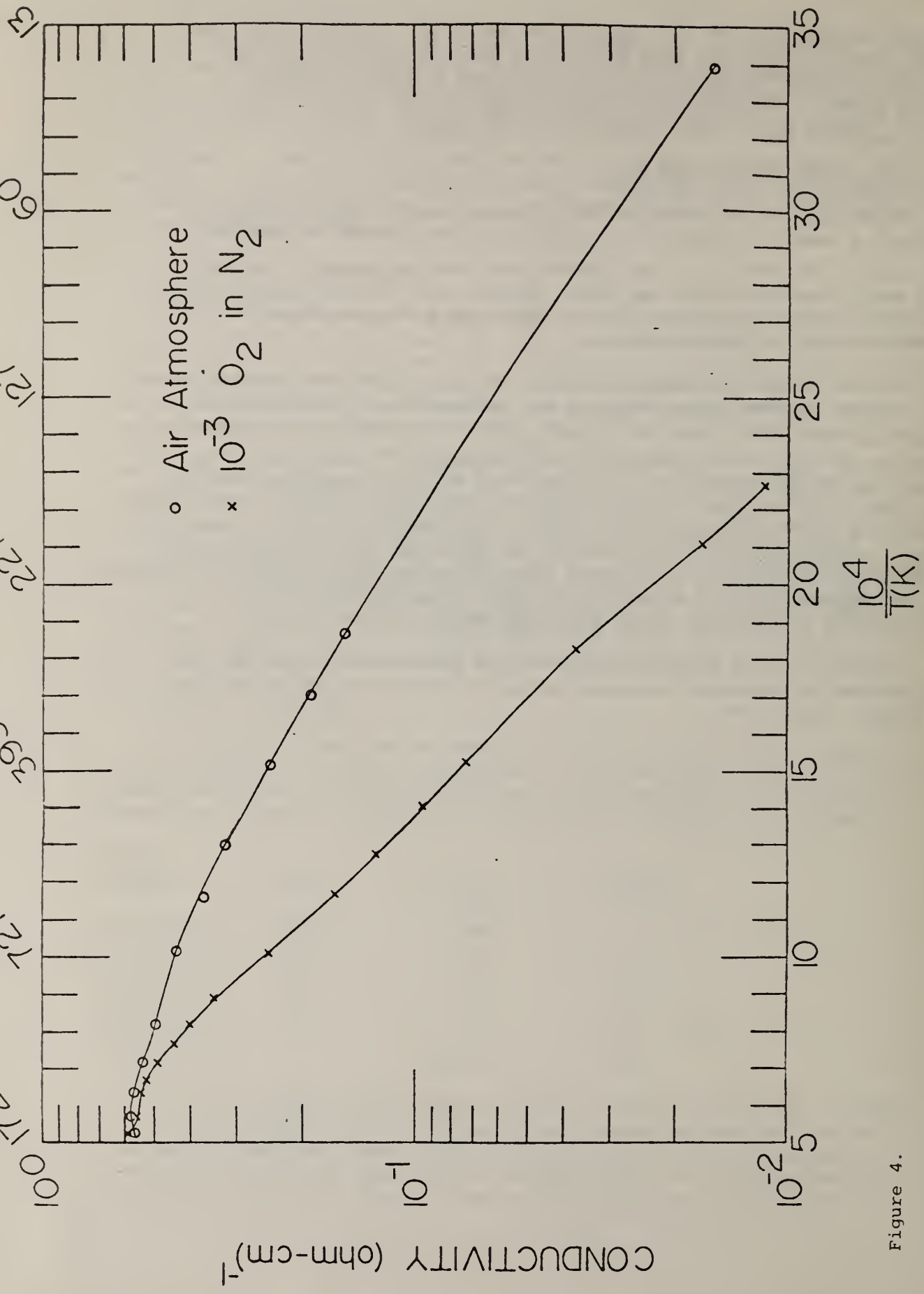


Figure 4.

Electrical conductivity of LaMg_{0.02}Al_{0.23}Cr_{0.75}O₃ as a function of temperature at several partial pressures of O₂. This sample was tested as part of Group II, Phase III U-02 Materials; it being the lower half of a two component electrode. The sample was prepared at Westinghouse Research and Development Center,

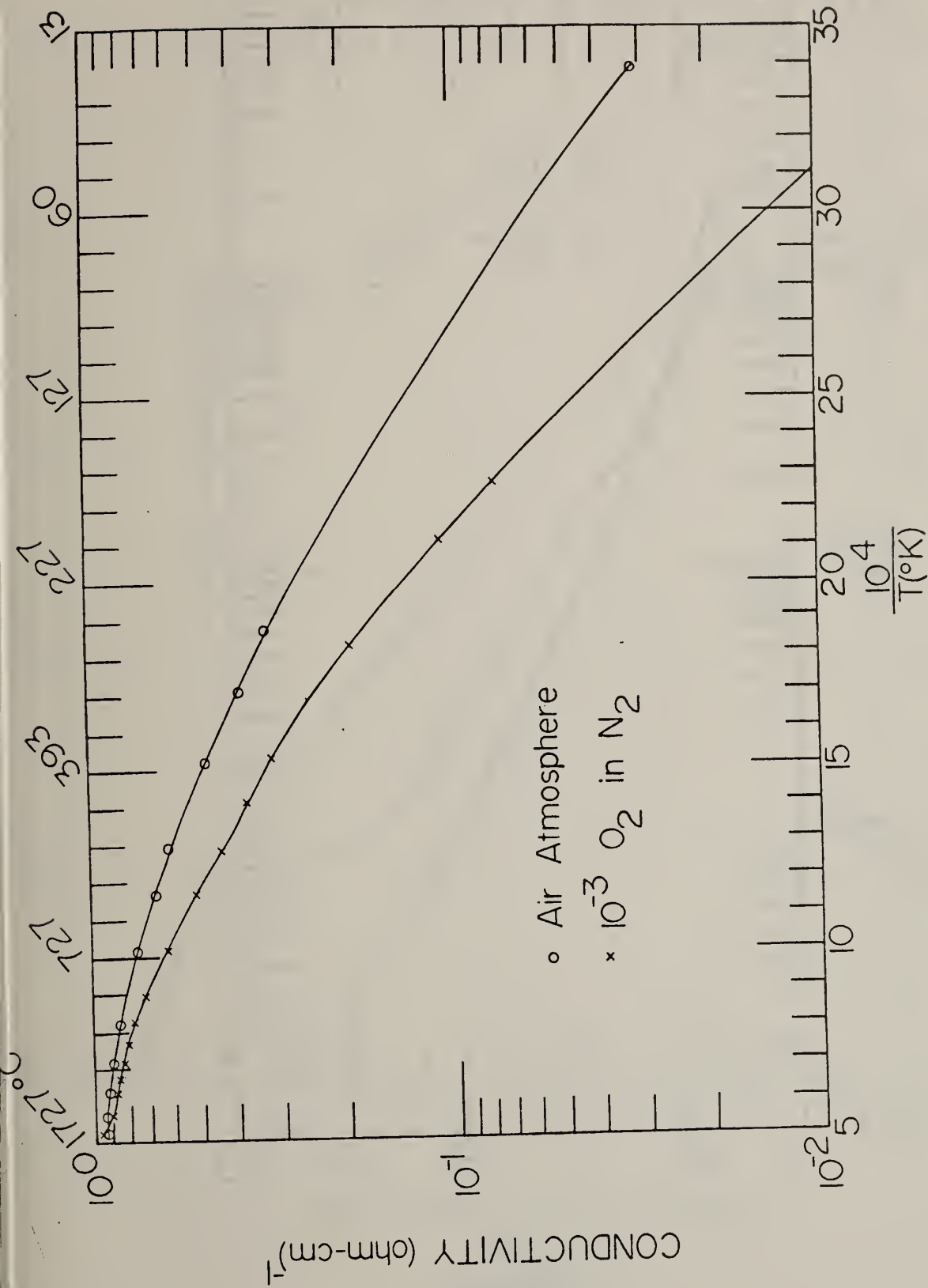


Figure 5.

Electrical conductivity of $\text{LaMg}_{0.02}\text{Al}_{0.13}\text{Cr}_{0.85}\text{O}_3$ as a function of temperature at several partial pressures of O_2 . This sample was tested as part of Group II, Phase III U-02 materials; it being the upper section of a two part electrode. The sample was prepared at Westinghouse Research and Development Center. (LC-AT-150(B)).

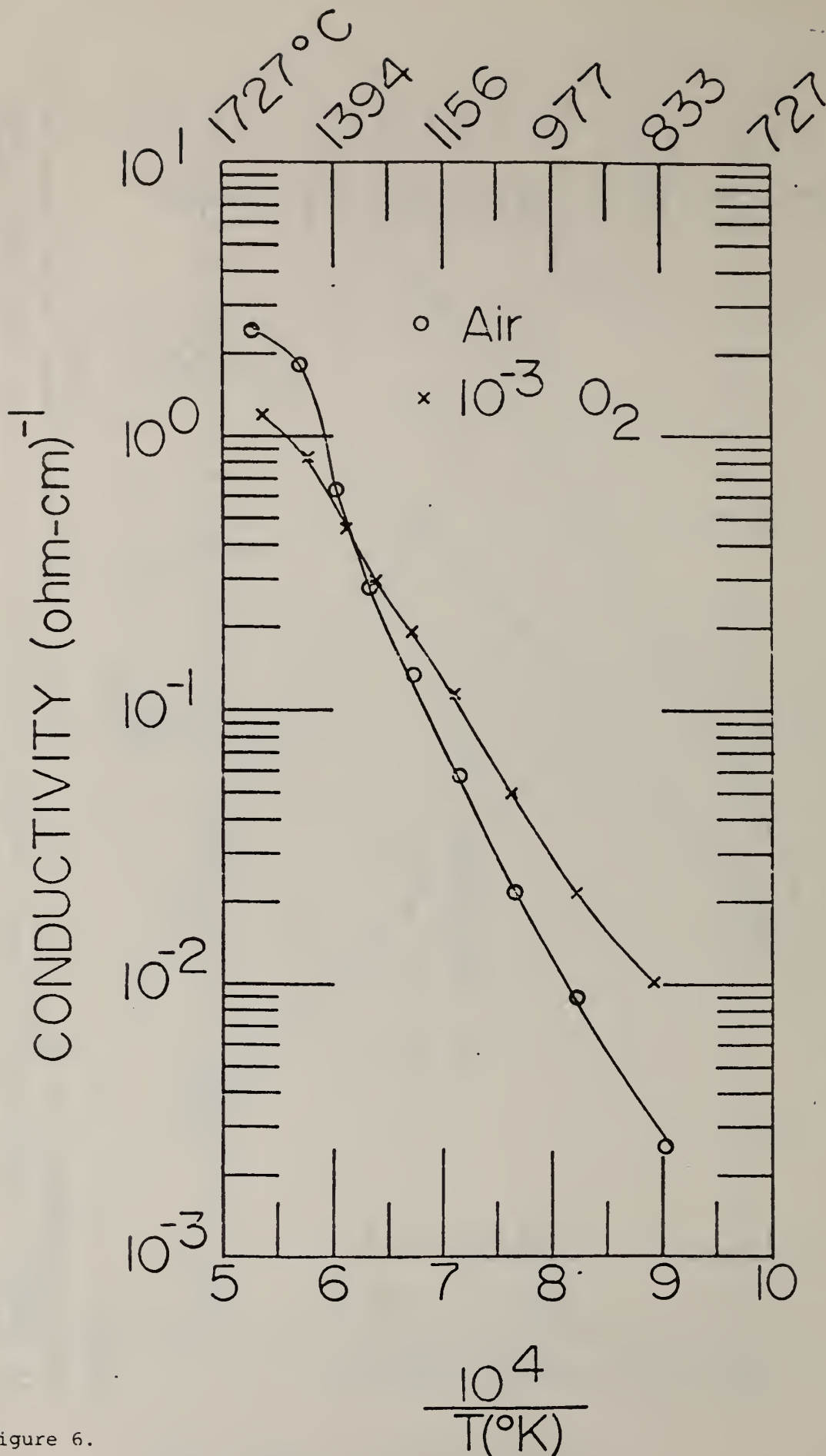


Figure 6.

Electrical conductivity of 60 m/o MgO-40 m/o Cr_2O_3 as a function of temperature at several partial pressures of O_2 . This sample, prepared at Westinghouse R & D Center was hot pressed at 3000 psi and 1650°C. (MC-AT-0501)

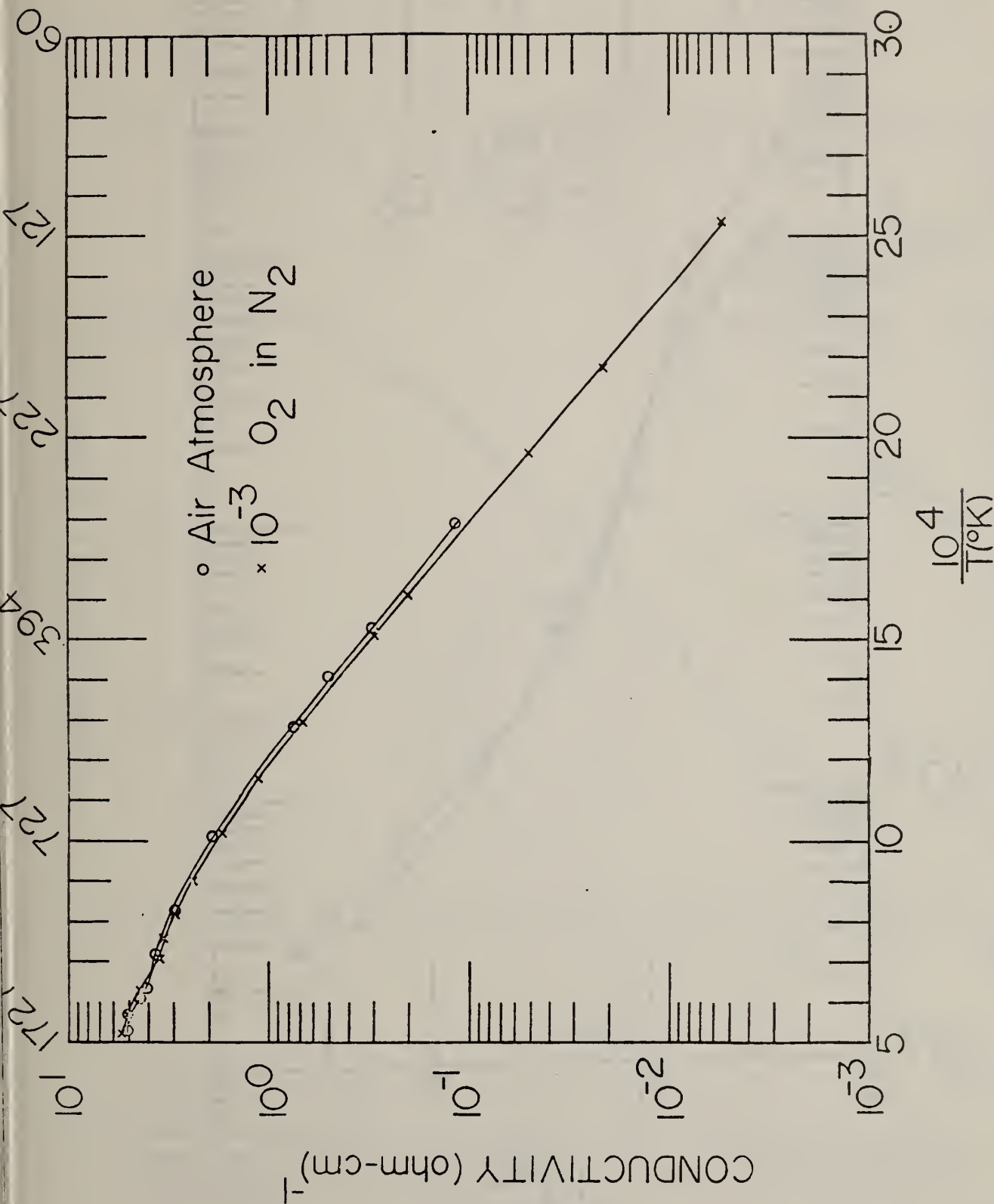


Fig. 7. Electrical conductivity of 56 m/o MgO-44m/o Cr₂O₃ as a function of temperatures at several partial pressures of O₂. This sample, prepared at Westinghouse R & D Center, was hot pressed at 3000 psi and 1650°C. MC-AT-0601

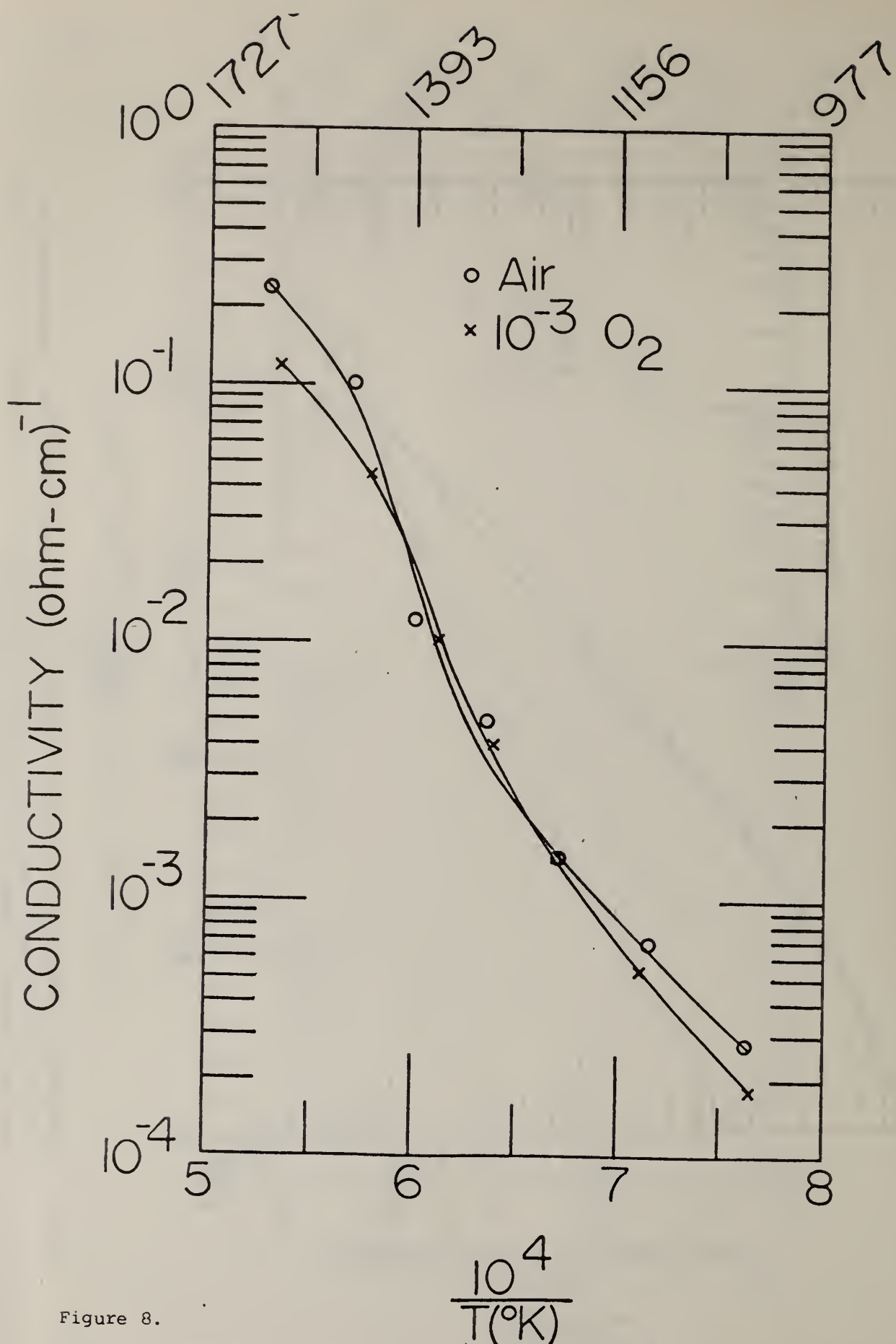


Figure 8.

Electrical conductivity of 52 m/o MgO-48 m/o Cr₂O₃ as a function of temperature at several partial pressures of O₂. This sample, prepared at Westinghouse R & D Center was hot pressed at 3000 psi and 1650 °C (MC-AT-0401).

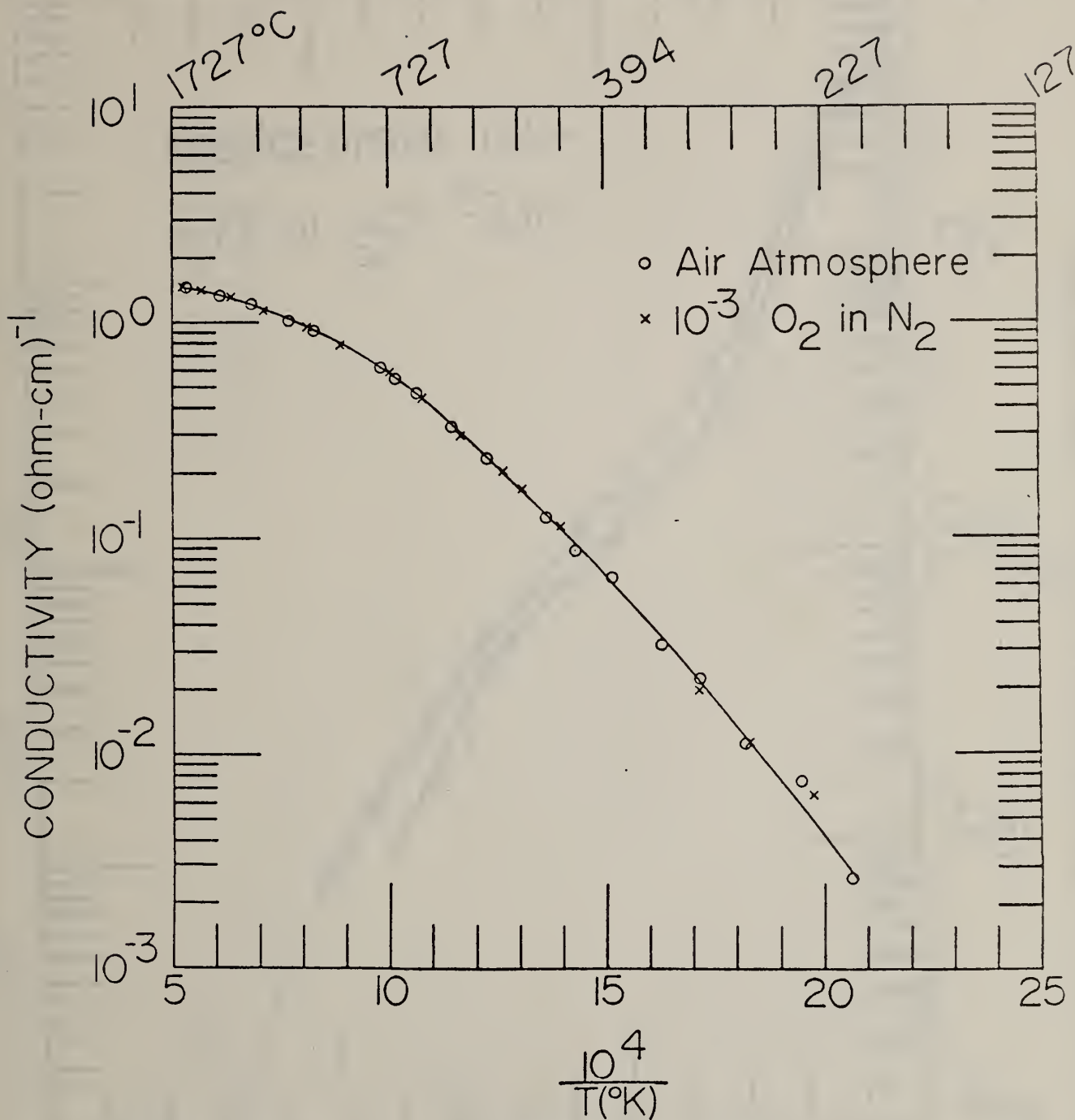


Figure 9.

Electrical conductivity at 50 m/o MgO - 50 m/o Cr_2O_3 as a function of temperature of several partial pressure of O_2 . This sample, prepared at Westinghouse R & D Center was hot pressed at 3000 psi and 1650 $^{\circ}\text{C}$. (MC-AT-0101).

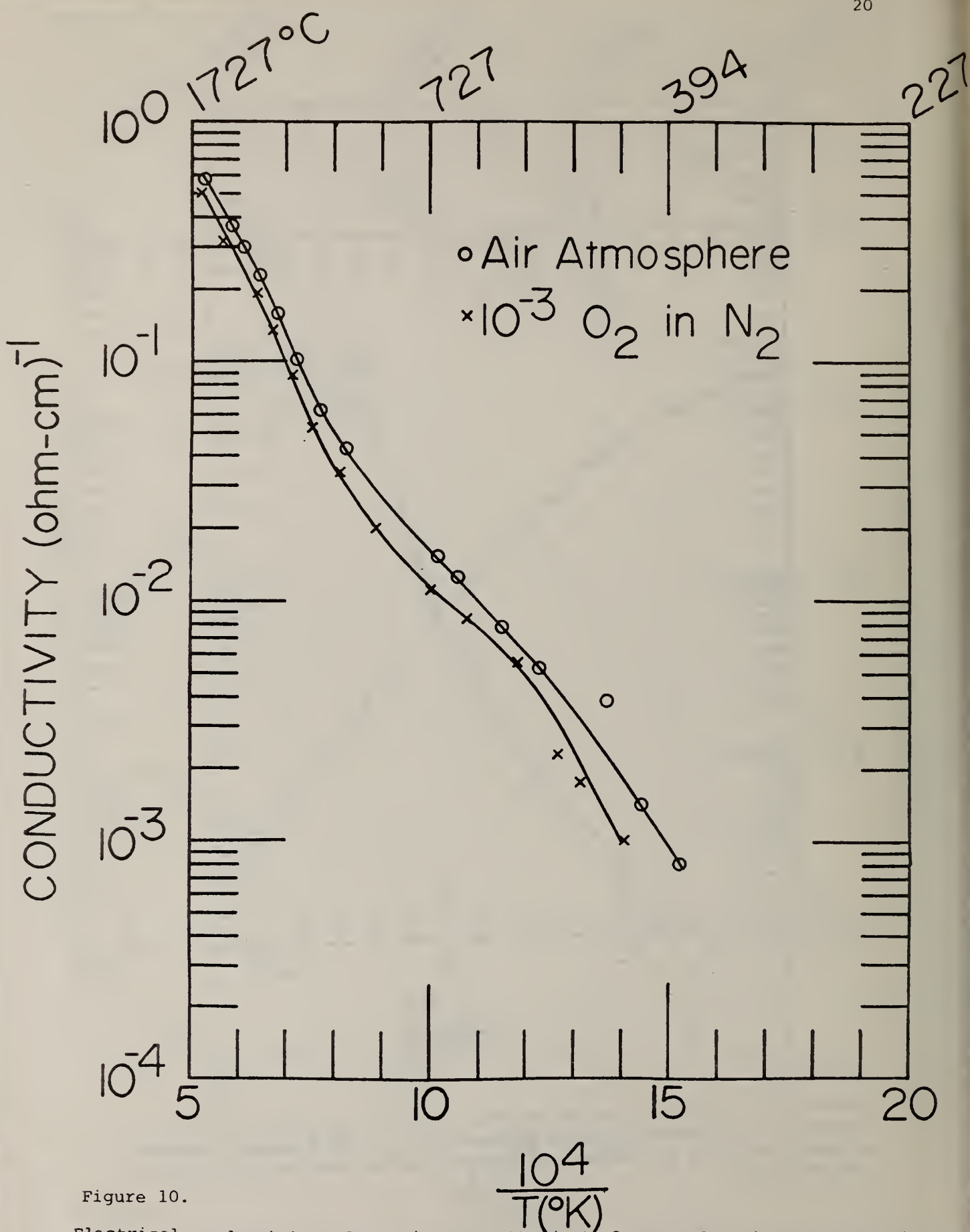


Figure 10.

Electrical conductivity of 48 m/o MgO - 52 m/o Cr₂O₃ as a function of temperature at several partial pressures of O₂. This sample, prepared at Westinghouse R & D Center was hot pressed at 3000 psi and 1650 °C. (MC-AT-0301).

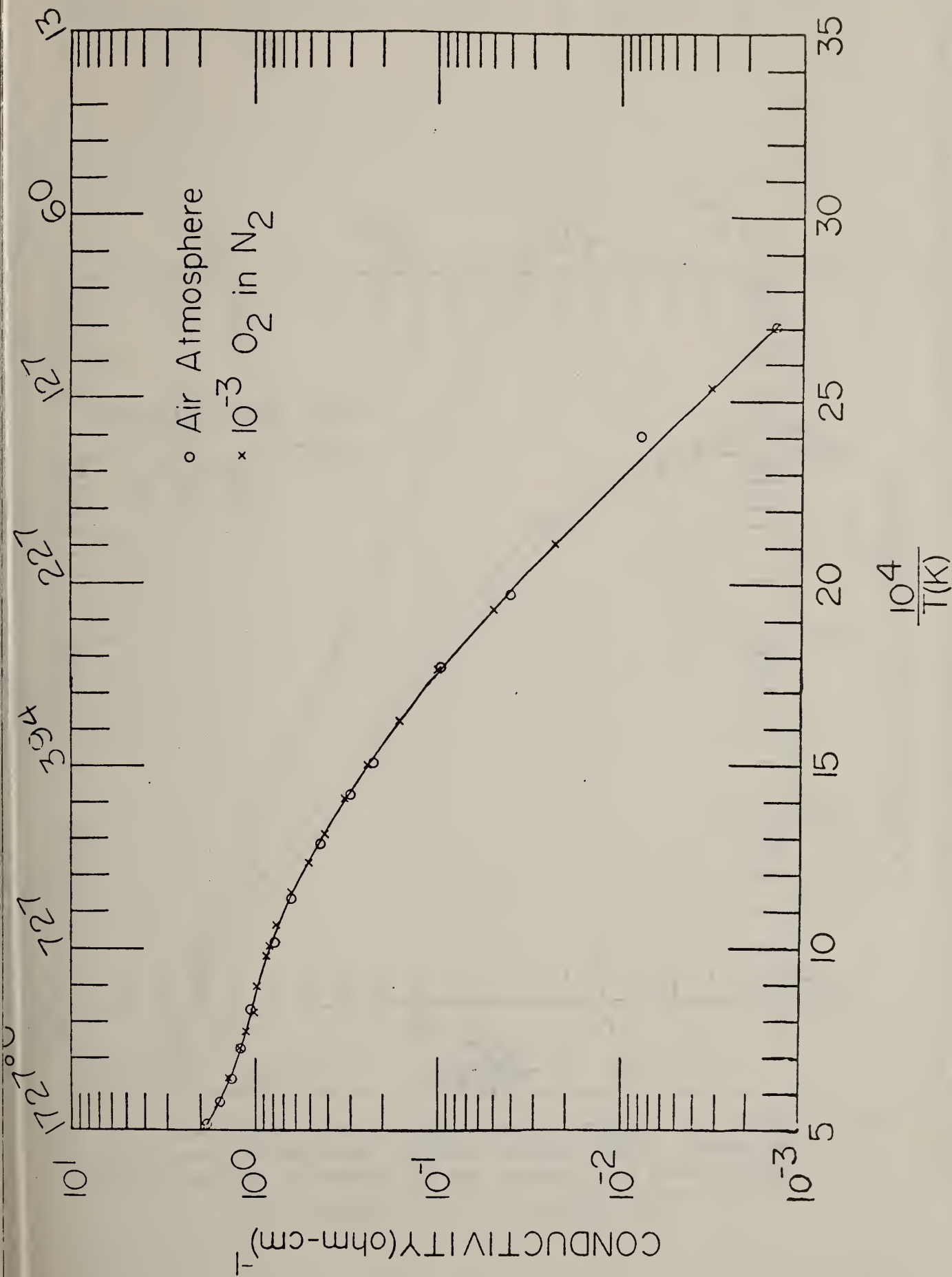


Fig. 11. Electrical conductivity of 98 m/o Cr₂O₃-2m/o MgO as a function of temperature at several partial pressures of O₂. This sample, prepared at Westinghouse R & D Center, was hot pressed at 3000 psi and 1650° MC - AT - 0701

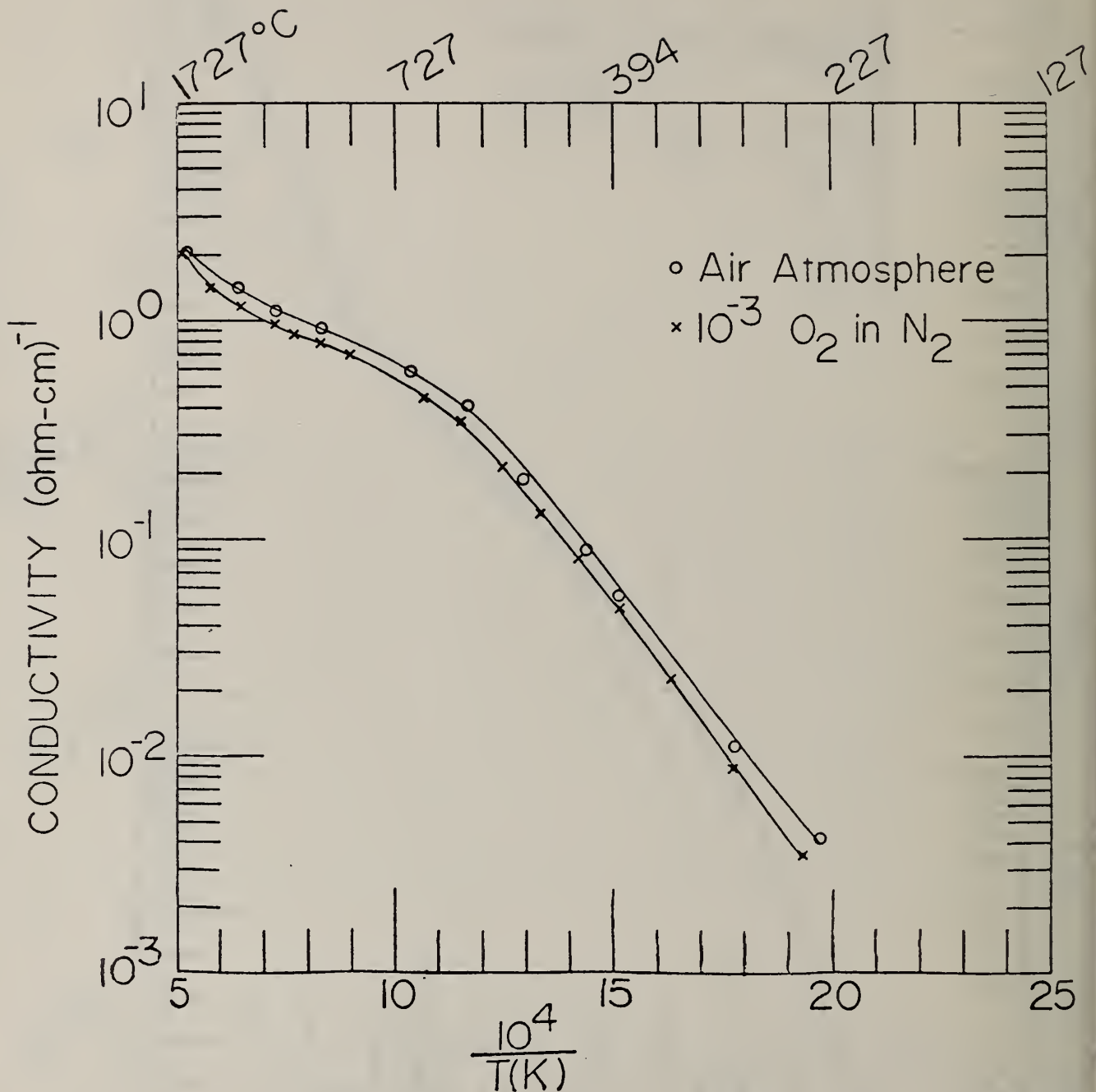


Fig. 12. Electrical conductivity of Cr_2O_3 as a function of temperature at several partial pressures of O_2 . This sample, prepared by Westinghouse R & D Center, was hot pressed at 3000 psi and 1450°C .
 CO - A1 - 0101

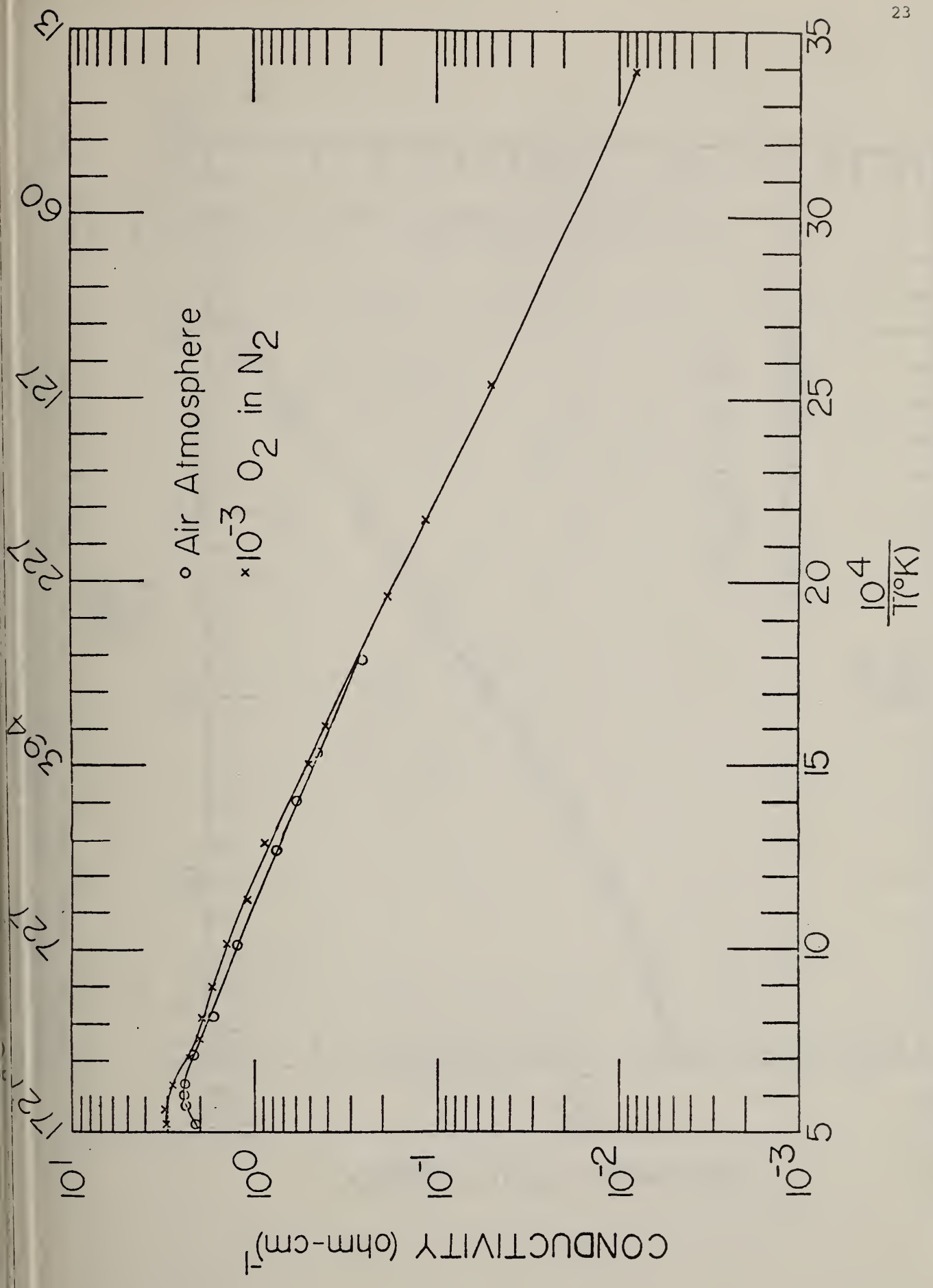


Fig. 13. Electrical conductivity of Y Mg 0.95 Cr 0.05 O₃ as a function of temperature at several partial pressures of O₂. This sample, prepared by Westinghouse R & D Center, was hot pressed at 3000 psi and 1650°C. (YC-AT-0101)

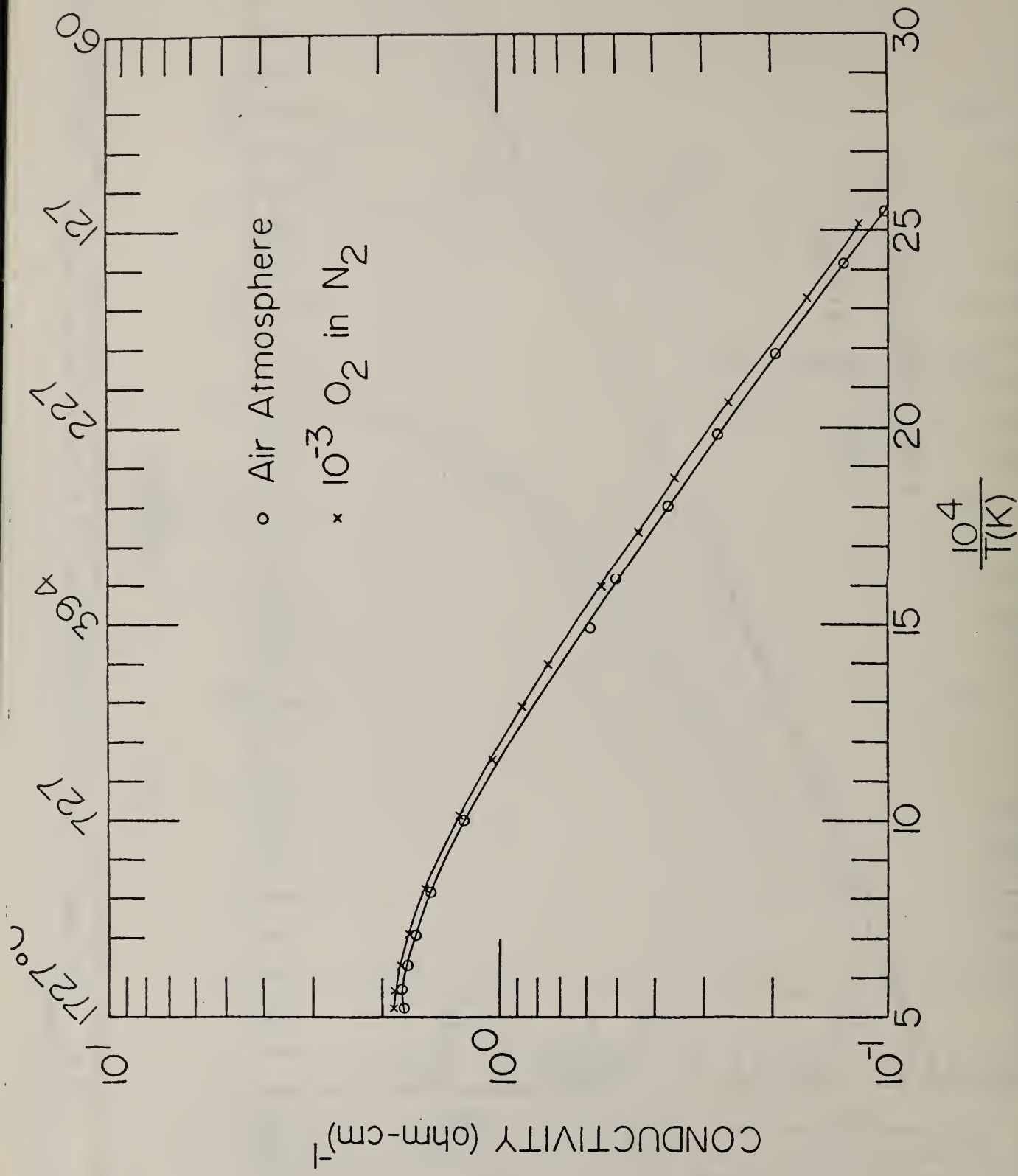


Fig. 14. Electrical conductivity of Y_{0.98}Ca_{0.02}CrO₃ as a function of temperature at several partial pressures of O₂. This sample was thermally sintered at 1746°C for 6 hours in forming gas, and was about 90.2% dense. TT-MS 8416

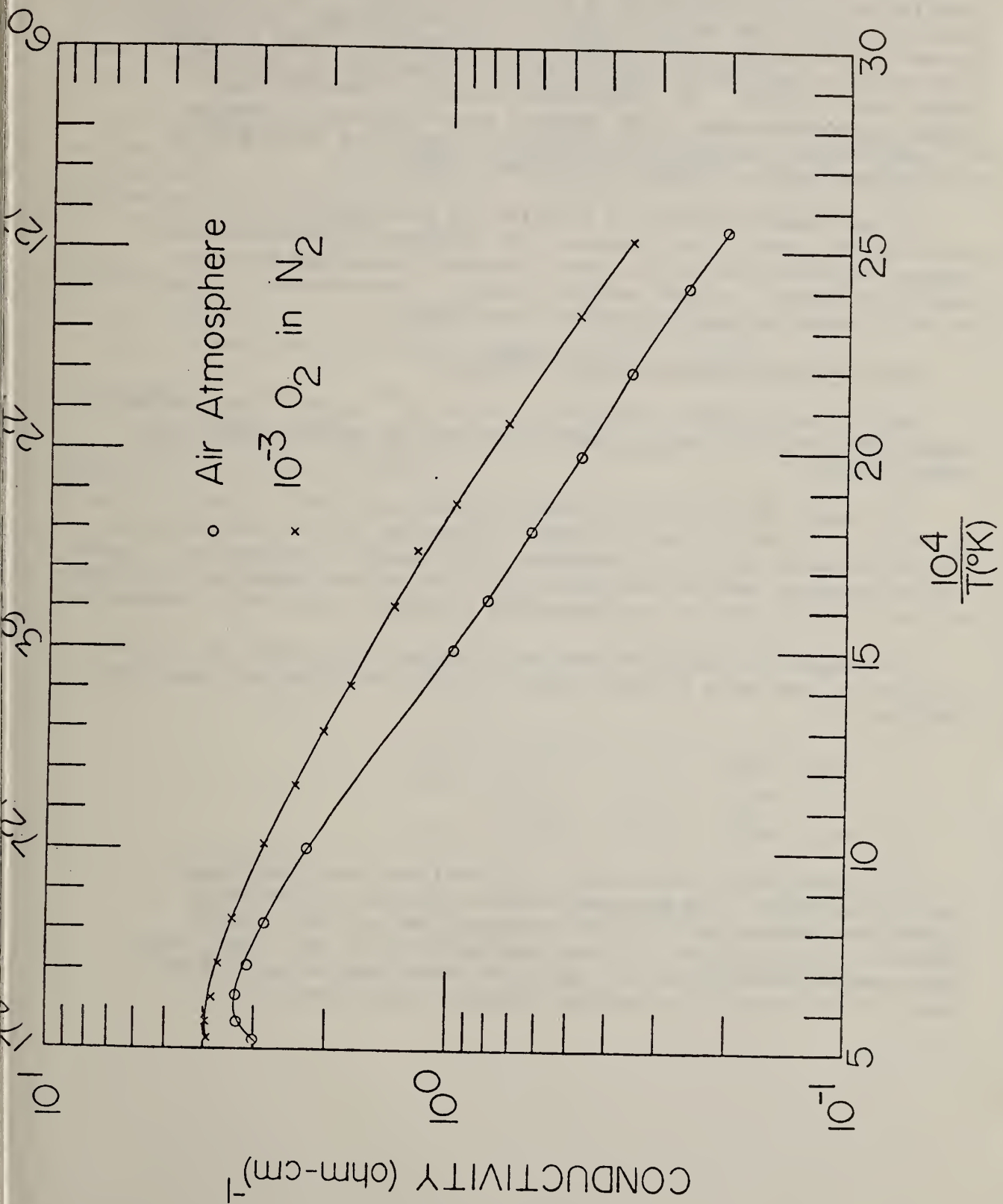


Fig. 15. Electrical conductivity of $\text{Y}_{0.95}\text{Ca}_{0.05}\text{CrO}_3$ as a function of temperature at several partial pressures of O_2 . This sample was thermally sintered in forming gas at 1746°C for 6 hours and was 95.2% dense. (TT-MS-8417)

3. Vaporization Studies (E. R. Plante)

Previous reports of vaporization studies have dealt extensively with measurements of the potassium gas pressure over K_2O -containing compounds or phases. These data are necessary for prediction and correlation of the interaction of a seeded MHD plasma with construction materials or cold ash using equilibrium thermodynamics. For example, Spencer (1) noted the severe lack of thermodynamic or vapor pressure data needed to model seed-slag interaction parameters in ternary or higher order systems. The vaporization studies at NBS have been planned to provide some of the required data as well as to measure K_2O activities in solutions having up to 6 components which will be more representative of slags in real MHD systems.

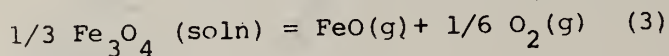
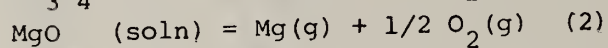
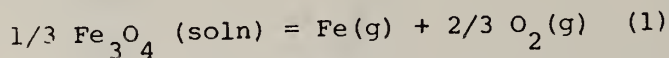
An additional objective of vaporization measurements is to determine the stability of potential MHD construction materials with respect to degradation due to loss of doping of materials by vaporization processes. In this quarter, results of measurements on the potential electrode material MAFF-31 are reported.

3.1 Vapor Pressure Measurements on "MAFF-31"

MAFF-31 has a spinel structure in which Fe^{+2} and Fe^{+3} ions randomly replace Mg^{+2} and Al^{+3} ions in spinel. It has the nominal composition $3MgAl_2O_4 \cdot Fe_3O_4$.

The sample was prepared by Trans-Tech and was fired at 1400 °C in air at NBS for 1/2 hour to remove binders. Since the MAFF-31 composition is a solid solution the partial pressures will depend on composition. During the measurements reported here less than 4 wt% of the sample was vaporized so that the pressures are representative of the 3:1 molar ratio composition.

The sample was vaporized from an Ir Knudsen cell having an orifice diameter of 1 mm and a Clausing factor of .41. The principal vaporization reactions are:



The measurements were made in our modulated beam, quadrupole mass spectrometer. The mass spectrometer constant for Fe^+ was determined assuming that the entire weight loss was due to evaporation of " Fe_3O_4 " which is a good approximation in this case. Mass spectrometer constants for O_2 , Mg and FeO were then estimated from relative ionization cross sections obtained from literature.

The data are shown in Figure 16. In order of decreasing pressure the lines represent the Fe(g), O₂(g), Mg(g) and FeO(g) pressures. It is interesting to note that measured Fe(g) and Mg(g) pressure are only 20 to 50% below the values that would be expected if Fe₃O₄ and MgO were at unit activity. This observation is consistent with the relatively low heat of formation of spinel from its component oxides (~ -10 kcal). The slope of the O₂(g) pressure curve is significantly less than the slopes of the other 3 curves. This is consistent with the fact that spinels tend to become oxygen deficient at higher temperatures.

At a temperature of 2000K the Fe pressure over the MAFF-31 composition is close to 10^{-5} atm. Under clean electrode conditions the rate of loss of Fe at 2000 K would be appreciable. However, electrode lifetime would be enhanced by a significant factor if electrode surface temperatures could be held in 1800-1900 K range.

Reference

1. F. E. Spencer, Jr., J. C. Hendrie, Jr., and D. Bienstock, 6th Intl. Conf. on MHD Power Generation, Washington, D. C. (1975).

Future Work

In the next quarter, measurements on the K(g) pressure over K₂O containing compositions will be continued.

VAPOR PRESSURE OF MAFF 31

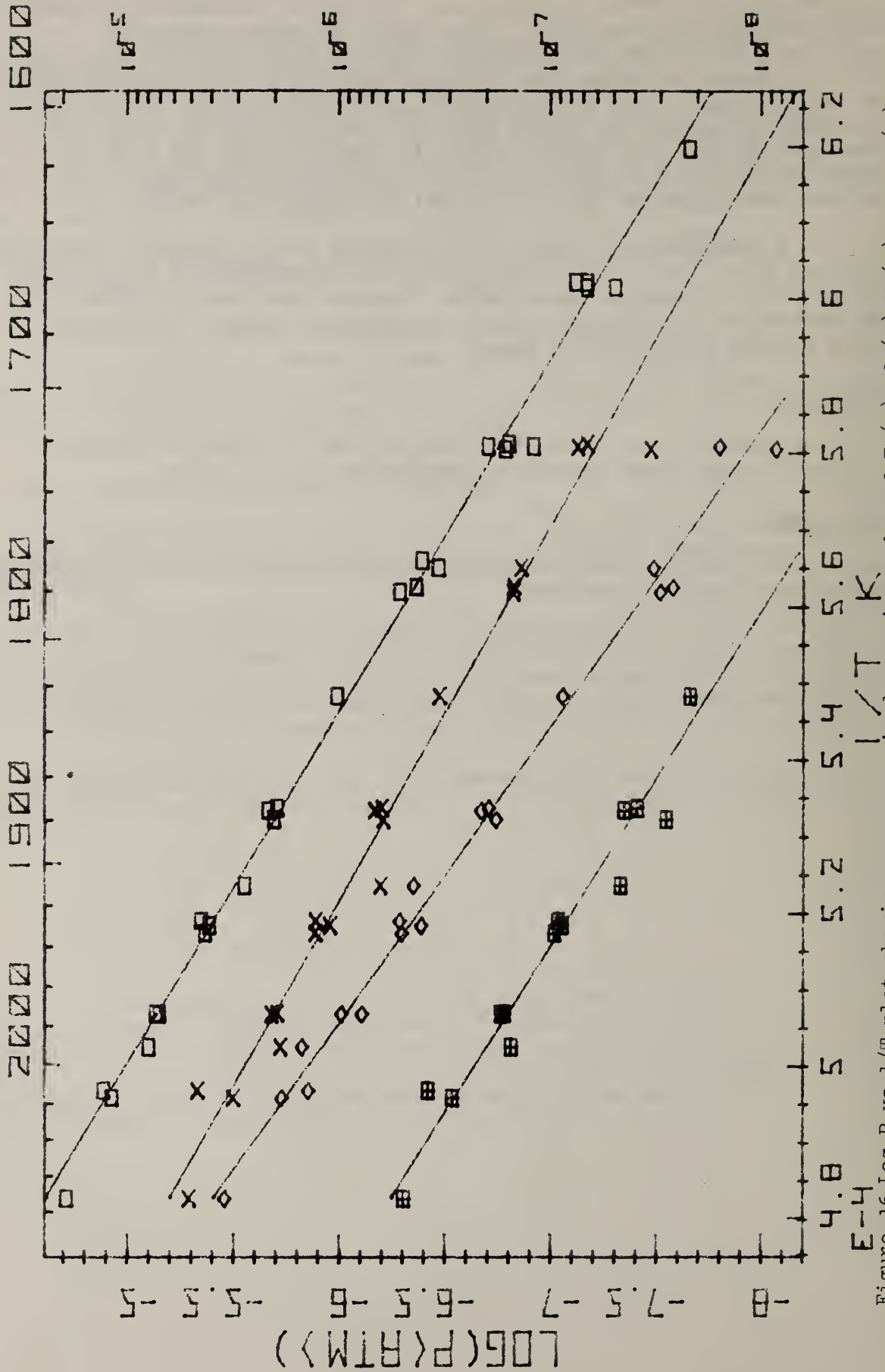


Figure 16. Log P vs 1/T plot showing pressures in decreasing order of Fe(g), O₂(g), Mg(g) and FeO(g) over MAFF-31.

TASK J. CORROSION AND DIFFUSION

1. Diffusion in Insulator-Electrode Couples (E. N. Farabaugh and J. R. Manning)

Interdiffusion of iron between MgO insulator material and MAFF 31 ($3\text{MgAl}_2\text{O}_4 \cdot 1\text{Fe}_3\text{O}_4$) at 1400 °C has been measured and analyzed. Combining these results with previous measurements of interdiffusion at 1600 °C (Quarterly Report Sept.-Dec. 1977, page 31) provides an estimate of the temperature dependence of diffusion in these materials. The concentration profile obtained from the 100 hr. test of 1400 °C for the MAFF 31-MgO couple is shown in Figure 1. In the plot, the complete profile is not reproduced because of the long tails in the MAFF and MgO. The figure shows the tail in the MAFF, the profile near the interface and the tail in the MgO.

Analysis of the interdiffusion results was done by plotting the concentration vs. distance points on probability paper. On such a plot, a single straight line would be obtained if the diffusion coefficient were constant. The probability plot indicated that there are three distinct diffusion regimes in the couple, each of which is characterized by a more-or-less linear segment on the probability plot. Near the original interface a sharp concentration gradient was found in iron concentration; whereas, by contrast, the gradients in the neighboring regions were noticeably much less sharp. Iron diffusion in the MgO was found to proceed about 3 times as fast as iron diffusion in the MAFF 31. The value of the iron interdiffusion coefficient in the MgO is approximately $12 \times 10^{-10} \text{ cm}^2/\text{sec}$ and that in the MAFF 31 is approximately $4 \times 10^{-10} \text{ cm}^2/\text{sec}$.

The sharp concentration gradient in the middle region corresponded to an effective diffusion coefficient of about $0.5 \times 10^{-10} \text{ cm}^2/\text{sec}$. This regime covered the composition range from about 30% to 75% of maximum iron concentration in the MAFF 31 and extended in distance from approximately the final position of the interface after diffusion to near the Matano interface position, or roughly the original interface location. Thus, this interface region may represent a transition regime between the original MAFF 31 and MgO sintered samples.

Because of the effective low diffusion coefficient, the interface region may provide a barrier to Fe diffusion from the MAFF 31 into the MgO; but within the MgO itself iron diffuses more readily than in the MAFF 31 spinel ($3\text{MgAl}_2\text{O}_4 \cdot 1\text{Fe}_3\text{O}_4$) structure. This difference occurs despite the MgO specimen being closer in density to the theoretical density value than the MAFF specimen (98% of theoretical density for the MgO vs. 95% for the MAFF). It is possible that in both the MgO and MAFF regions grain boundary diffusion is strongly influencing the results that are observed.

When the present results are compared with previous results on interdiffusion in MAFF 31-MgO samples at 1600 °C, it is found that the increase in temperature from 1400 °C to 1600 °C increases the diffusion coefficient in all three regions of the couple by a factor of approximately 4 to 7. Since the penetration distance of the iron into the MgO and the extent of the iron depletion region in the MAFF are proportional to the square root of the diffusion coefficient, the penetration distance for iron diffusing out of the MAFF electrode material and into the MgO insulator materials is increased by approximately a factor of 2 to 2-1/2 when the temperature is increased from 1400 °C to 1600 °C.

Similar factors of increase in diffusion coefficient and penetration distance would be expected if the temperature were increased for example to 1800°C, with the penetration doubling about every 200C deg., presuming no change in diffusion mechanism. Large extrapolations become increasingly doubtful, however, both because some change in diffusion mechanism probably will occur as temperature is increased, thus changing the temperature dependence, and because the temperature dependence even in the region 1400°C to 1600°C still is not known with great accuracy.

At the end of 100 hours at 1400°C, penetration of Fe into the MgO is about 600µm and from the MAFF about 300µm. According to theory, diffusion penetration is expected to be proportional to the square root of the time. Thus, penetration after 400 hours would be double those shown in the figure. This dependence on time was confirmed for the present materials in the measurement made at 1600°C, and similar results are presumed to be valid at other nearby temperatures, again presuming no major change in the reactions that are occurring. Thus, present results allow estimates to be made of total penetration expected for not only other temperatures but also other times. Further measurements underway on a similar couple diffused at 1500°C will provide more detailed information on the temperature dependence.

MAFF31-MgO and MAFF31-S71 ($MgAl_2O_4$) diffusion couples tested at 1500°C for 30 hrs. each have been prepared. Profiles for these couples and their analysis will be presented in the next quarterly report.

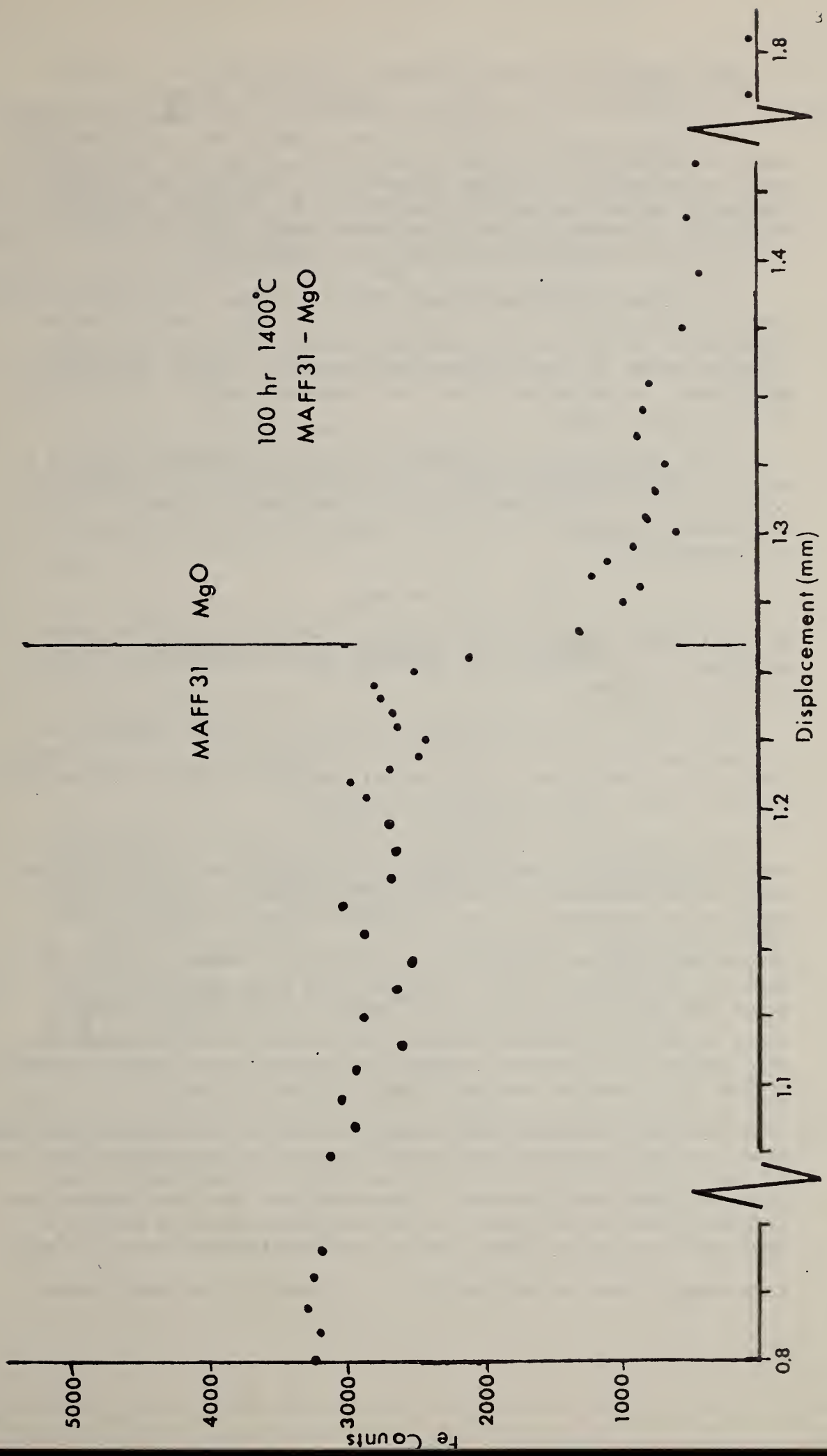


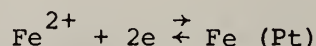
Figure 1. Fe concentration profile in MAFF31-MgO diffusion couple tested at 1400°C for 100 hrs.

2. High Temperature Charge Transport in Coal Slags (K. F. Young, A. D. Franklin, N. K. Adams, L. Hsu and C. K. Chiang)

The furnace described in our Quarterly Report for April-June 1978 (EA-77-A-01-6010-12) describes a platinum-wound furnace for electrical measurements on slags at high temperatures. This furnace has been completed, tested and put into operation. The maximum operational temperature is about 1550 °C. The temperature variation over the region of the furnace occupied by the specimen is less than 1 °C.

Preliminary measurements have begun on a sample of synthetic slag K302 (the composition of this slag is given in the Quarterly Report cited above) at a relatively low temperature, around 1250 °C. The slag was broken up with a hammer and placed as a powder around the electrodes. As described in our last Quarterly Report, one electrode was Pt and the other Fe.

Under open circuit conditions a voltage is observed, with the Fe negative, whose magnitude drops slowly with time from more than 0.4 V to around 0.1 V. Under short circuit conditions a current of 0.1 to 2 mA flows. Evidently, the electrochemical reaction of iron at the Pt electrode



is sufficiently rapid that the cell can act as a battery. The Pt in parenthesis at the right side indicates that the Fe dissolves into or alloys with the Pt.

The drop off in open-circuit potential with time suggests that at least the surface of the Pt becomes saturated with Fe, even under open-circuit conditions. This can only occur if transport in the slag by both Fe ions and by electrons is possible.

When a potential difference was applied across the electrodes, zero current occurred when the applied potential exactly matched this open circuit potential. With the Fe more negative than this, ohmic behavior was observed for over potentials of up to several volts. This current should be purely electronic, although conceivably dischargeable anions could also carry current. However, oxygen ions appear to be the only viable candidate, and these experiments are being done under tank Ar ($P_{\text{O}_2} < 10^{-3}$ atm.) so that oxygen transport seems unlikely. At higher voltages the current increased more rapidly than linearly with voltage, suggesting that additional charge transport or transfer mechanisms are activated at higher voltages.

With the Fe positive with respect to the Pt the behavior again was ohmic for small over voltages, with a slope indistinguishable from that for the opposite polarity. Since this current should contain both electronic and ionic currents, it may mean that the ionic conductivity is much less than the electronic, a not unexpected state of affairs at temperatures not much higher than the melting temperature of the slag.

A systematic study of this behavior is planned for the next Quarter.

3. Electrochemical Effects in Simulated Slag Flow (E. N. Farabaugh, W. R. Hosler, W. Capps)

Previous work on "hot" platinum electrodes in a simulated slagging generator have been described in the last Quarterly Report (April - June 1978, page 31). Several of these electrodes have now been examined by SEM and EDX techniques. The results presented here cover the examination of the first two (E5 and E6) runs which were made using fly ash but no seed at a temperature of 1400°C. A brief summary of these results is given below.

E-5; rotor--cathode, stator--anode. (See April - June 1978, page 33 for photos of stator and roter).

- 1) The Fe had alloyed to some degree with the cathode. There was a high Fe concentration in the platinum at the cathode-slag interface. The concentration of Fe drops off towards the interior of the cathode. No Fe was detected in the anode.
- 2) No Fe-rich layer was found next to either the cathode or anode.
- 3) The cathode had a very porous microstructure at the cathode - slag interface. The anode exhibited the same type porous layer at the anode - slag interface, only thinner.
- 4) The slag was, in general, richer in Fe around the cathode than the anode.

E-6; rotor--anode, stator--cathode.

- 1) No Fe was detected in either the cathode or anode.
- 2) A thin Al-rich slag phase layer was found at the cathode-slag interface. Clumps of an Al-Fe-Cr phase were observed at the cathode-slag interface also.
- 3) No layer or clumps were seen at the anode-slag interface.
- 4) A porous microstructure layer was seen in the electrode at both the cathode-slag and anode-slag interfaces, thinner in the anode.

Runs 7 and 8 will be studied by SEM and EDX techniques and a complete analytical discussion of the results of runs 5,6,7 and 8 will be made in the next Quarterly Report.

4. Seed/Slag Interaction and Slag Corrosion (L. P. Cook)

Six-component synthetic "Eastern" and "Western" channel slags¹ with the compositions given in Table 1 were prepared according to the following treatment. Crystalline KAlO_2 , Mg_2SiO_4 and Ca_2SiO_4 were prepared by calcining the necessary reagents², with repeated⁴ homogenization, until x-ray powder patterns indicated complete reaction to produce the desired phase. These materials, with Fe_2O_3 and $\alpha\text{-SiO}_2$, were weighed in the appropriate proportions in a drybox³, homogenized under acetone, dried at 160°C under vacuum, and dry-homogenized repeatedly while hot. Pellets of 1/2" diameter were pressed, wrapped in Au foil, and fired at 950°C in air for 24 hrs. The products were brick red, indicating very little reduction. These pellets were crushed, re-pressed, wrapped in Pt foil, dried briefly at 950°C and weighed. They were then fired in air at 1300°C for 24 hrs, with periodic weighings. The model Eastern channel slag lost 17 mg, almost entirely within the first 3 hrs - in view of the high Fe content, this may represent predominately reduction. The model Western channel slag lost 9 mg continuously over the 24 hrs of heat treatment - this probably represents K_2O loss. Such weight losses indicate negligible K_2O vaporization in view of the 10 g total weight. Following this the products (now dark brown) were crushed, re-pressed, wrapped in Pt foil and refired at 1300°C in air for 36 hrs. Both compositions showed slight evidence of melting during the final heat treatment. X-ray powder patterns indicate that KAlSiO_4 is by far the dominant phase in both the Eastern and Western compositions⁴ as prepared. The Eastern composition contains as well small amounts of KAlSi_2O_6 and at least one unidentified phase. The Western composition also contains at least one other unidentified phase, presumably a calcium (iron, magnesium) silicate.

Following this mode of preparation, small samples were sealed in Pt tubes and equilibrated for varying lengths of time (see Table 2), then quenched. Polished surfaces were prepared and examined with SEM/EDX. By comparison with known standards, semiquantitative estimates of elemental compositions of various phases could be made.

Results for the "Eastern" channel slags are shown in Figures 2-8. As Figure 2 shows, there is evidence for two liquid phases in the "Eastern" model channel slag under the relatively oxidizing conditions in which these experiments were performed (10^{-1} to 10^0 atm P_{O_2}). Small globules of iron-rich melt can be seen adhering along the O_2 interfaces between crystalline KAlSiO_4 and the main melt phase, both at 1600°C where there is no Fe_3O_4 (Figure 2-A) and at 1475°C (Figure 2-B) below the precipitation temperature of Fe_3O_4 . These droplets appeared to coalesce slightly in some of the experiments, but location of droplets large enough for x-ray analysis was difficult. The semiquantitative analyses of the immiscible phase in Figures 3-8 must therefore be regarded with due caution, as the possibility of some contribution from surrounding phases cannot be completely discounted.

For this model "Eastern" channel slag composition, the iron-rich immiscible melt disappears below 1450°C and Fe_3O_4 spinel becomes correspondingly more abundant. These experiments indicate the relatively low amount (Figure 7; 15-20 wt % Fe as Fe_2O_3) of FeO which can be accommodated by the model "Eastern" channel slag under oxidizing conditions before supersaturation with respect to an iron-rich phase occurs. This has probable application to generator operation (anode side). Analogous experiments at low P_{O_2} (cathode) are planned. Model "Eastern" channel slag contained an appreciable volume % of crystals at 1625°C. The liquidus temperature although not determined, is thought to be above 1700°C. As KAlSiO_4 crystallizes with falling temperature, the main residual melt phase becomes depleted in K_2O (Figure 3). Al_2O_3 changes only slightly with falling temperature (Figure 4), and SiO_2 actually increases slightly in the residual melt (Figure 5). Calcium oxide shows a rather marked increase from ~3 wt % at 1575°C to ~10 wt % at 1325°C (Figure 6). Iron oxide in the main melt phase (Figure 7) increases slightly as the temperature falls from 1625°C to 1475°C, where an inflection in the fractionation curve (possibly corresponding to the precipitation of Fe_3O_4) results in decrease of iron content with further drop in the temperature to 1325°C. Magnesium oxide is present at low levels such that analytical uncertainty possibly accounts for some of the scatter in Figure 8. Compositions of the immiscible iron-rich melt phase are also plotted for the range 1550-1625°C. Significant K_2O , Al_2O_3 , and SiO_2 are present, but in considerably smaller percentages than FeO . CaO and MgO are definitely enriched in the immiscible melt phase relative to the main melt phase. The upward temperature termination of the postulated immiscibility field is not known; note the suggestion for a trend toward convergence of the two melt compositions above 1575°C.

Analogous experiments for the "Western" model channel slag are reported in Figures 9-14. In contrast to the "Eastern" model composition, no liquid immiscibility was observed, and the fractionation trends can be interpreted largely in terms of the crystallization of KAlSiO_4 , with resultant depletion of K_2O (Figure 9), Al_2O_3 (Figure 10), and SiO_2 (Figure 11) in the residual melt. Concomitant enrichment in CaO (Figure 12), FeO (Figure 13), and MgO (Figure 14) occurs within the residual melt as the temperature falls.

¹ E. R. Plante and L. P. Cook, "Compositional Modeling of MHD Channel Slag, with Preliminary Vapor Pressure Data", Proc. 17th Symp. Eng. Aspects MHD, Stanford, Calif., C.1.1 (1978).

Table 1. Suggested Compositions for Modeling Channel Slag.

	<u>Bituminous ("Eastern")</u>	<u>Sub-bituminous and Lower Rank ("Western")</u>
	wt % (Fe as Fe ₂ O ₃)	wt % (Fe as Fe ₂ O ₃)
SiO ₂	36.0	34.7
Al ₂ O ₃	25.5	24.5
CaO	1.8	9.3
MgO	0.6	3.3
K ₂ O	<u>23.6</u>	<u>22.7</u>
	100.0	100.0

Table 2. Quench Experiments on Model Channel Slags.

<u>Composition</u>	<u>T°C</u>	<u>Duration (h)</u>	<u>Composition</u>	<u>T°C</u>	<u>Duration (h)</u>
Eastern	1200	48*	Western	1200	48*
"	1225	46*	"	1225	46*
"	1250	23.5*	"	1250	23.5*
"	1275	24*	"	1275	24*
"	1300	24*	"	1300	24
"	1325	10.5	"	1325	10.5
"	1350	8	"	1350	8
"	1375	21	"	1375	21
"	1400	6	"	1400	8.5
"	1425	5	"	1425	5
"	1450	4	"	1450	4
"	1475	2	"	1475	2
"	1500	2.5	"	1500	2.5
"	1525	1	"	1525	1
"	1550	2.5	"	1550	2.5
"	1575	2.5	"	1575	2.5
"	1600	1	"	1600	1
"	1625	1			

* Not enough melt phase present for analysis.



A



B

Figure 2. High contrast secondary electron images of polished surfaces, quenched model "Eastern" channel slag ($\sim 4500\times$). K = KAlSiO_4 , KAlSi_2O_6 ; M = main residual slag phase; I = immiscible iron-rich melt; F = iron spinel; R = raster mark, showing size of EDX analysis area.

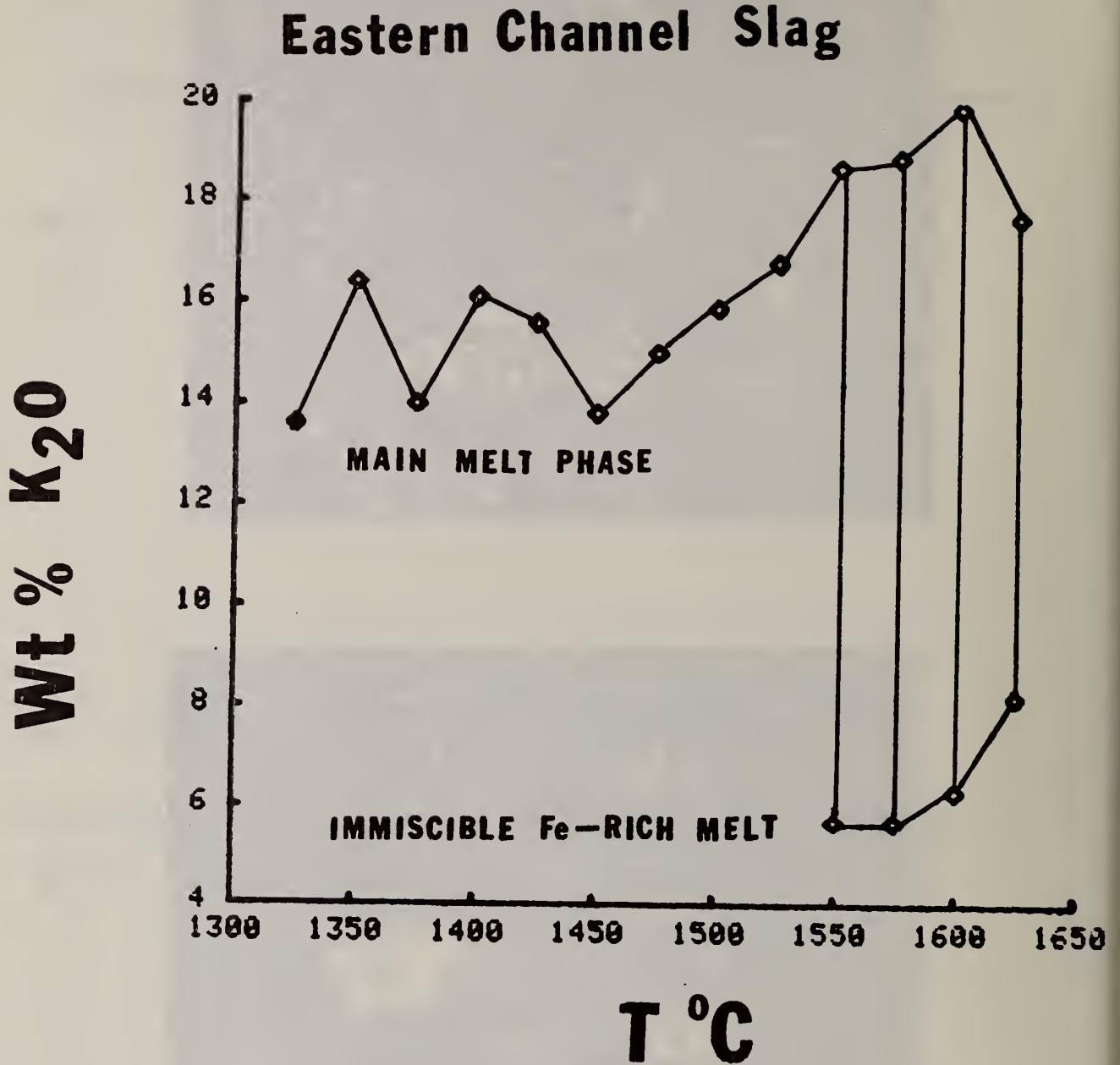
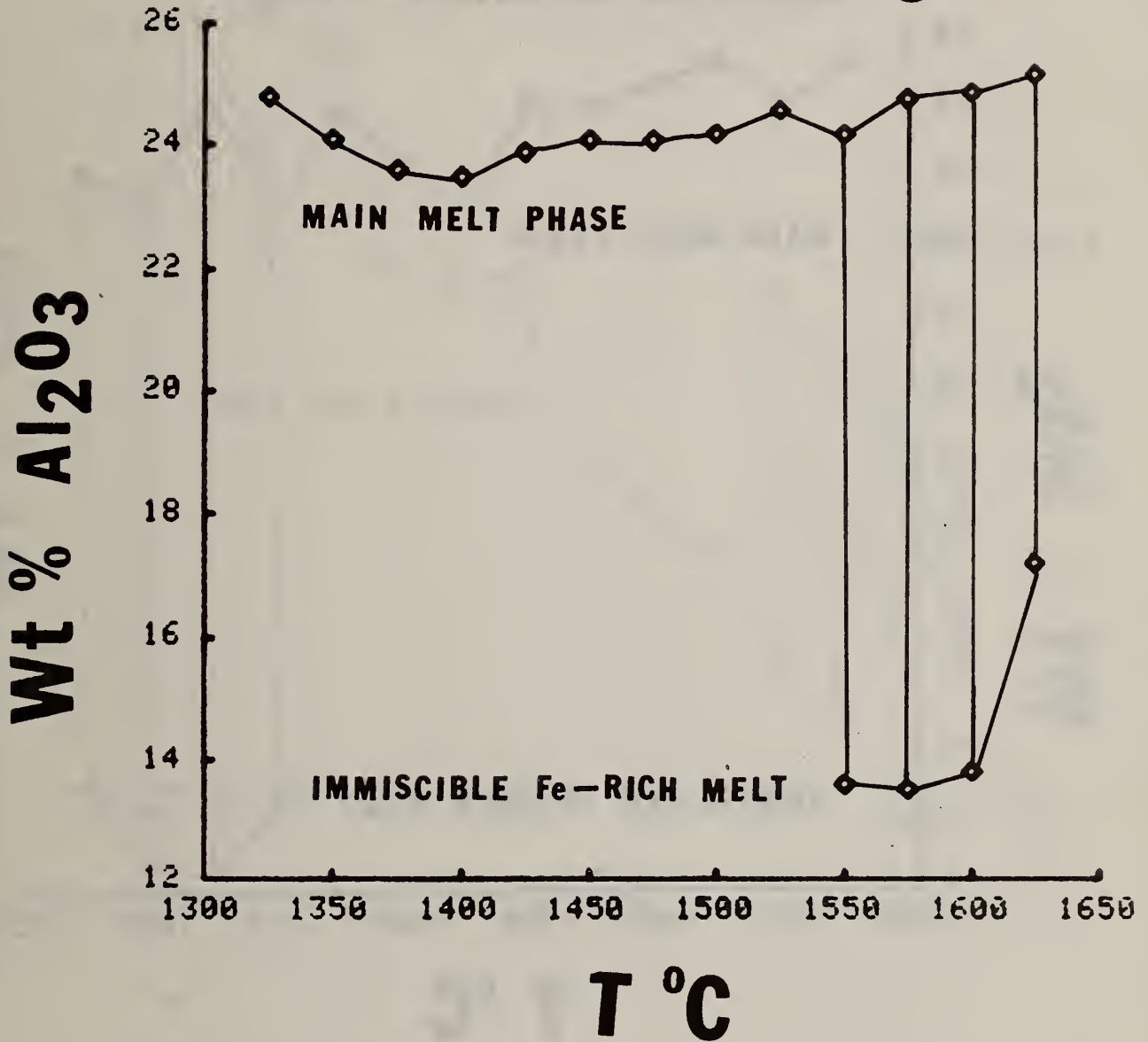


Figure 3. Semiquantitative analyses (I/I) of wt % K₂O as a function of T(°C) in residual slag phases for model "Eastern" channel slag composition.

Eastern Channel Slag



4. Semiquantitative analyses (I/I) of wt % Al_2O_3 as a function of T ($^\circ\text{C}$) in residual slag phases for model "Eastern" channel slag composition.

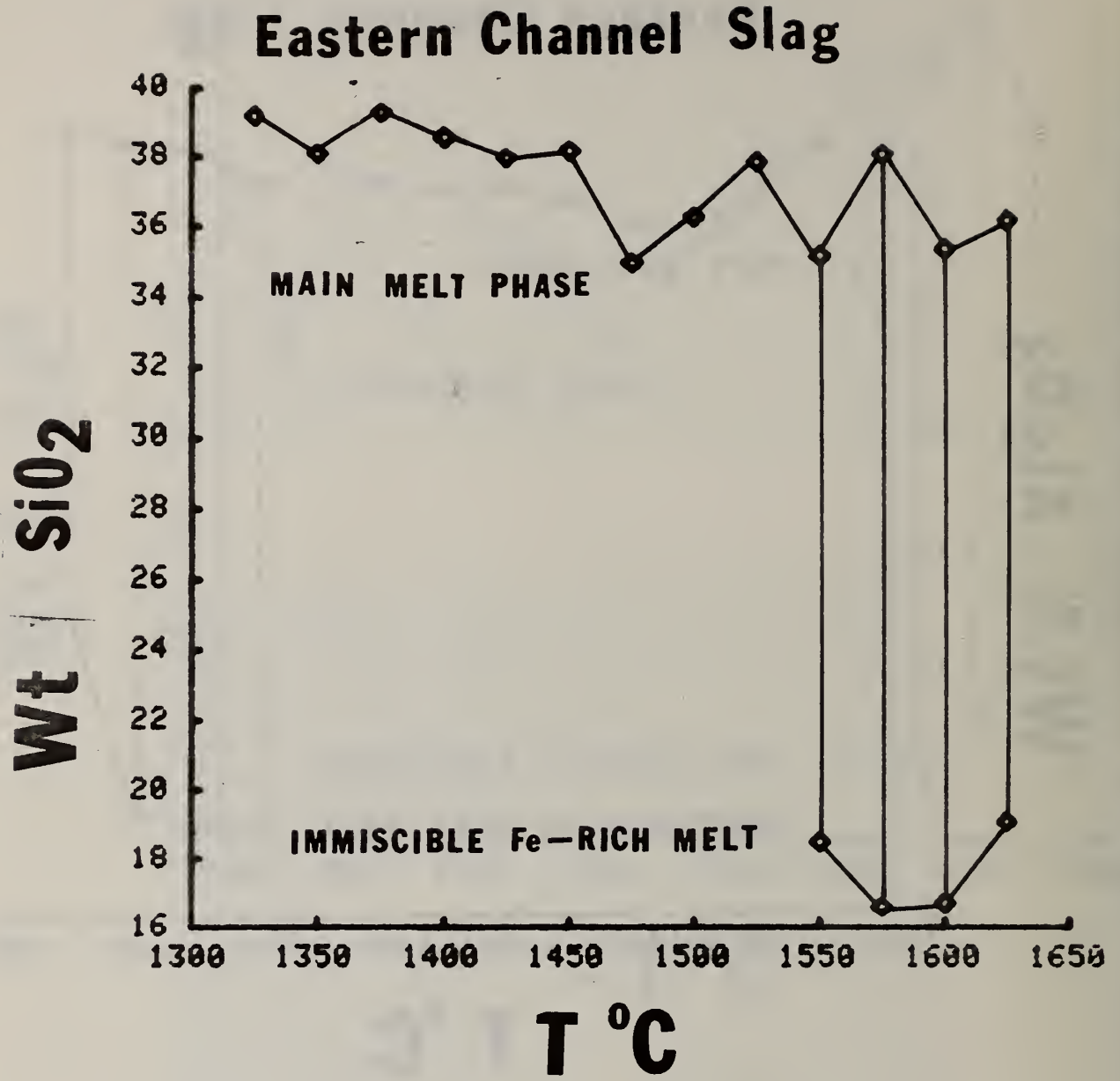
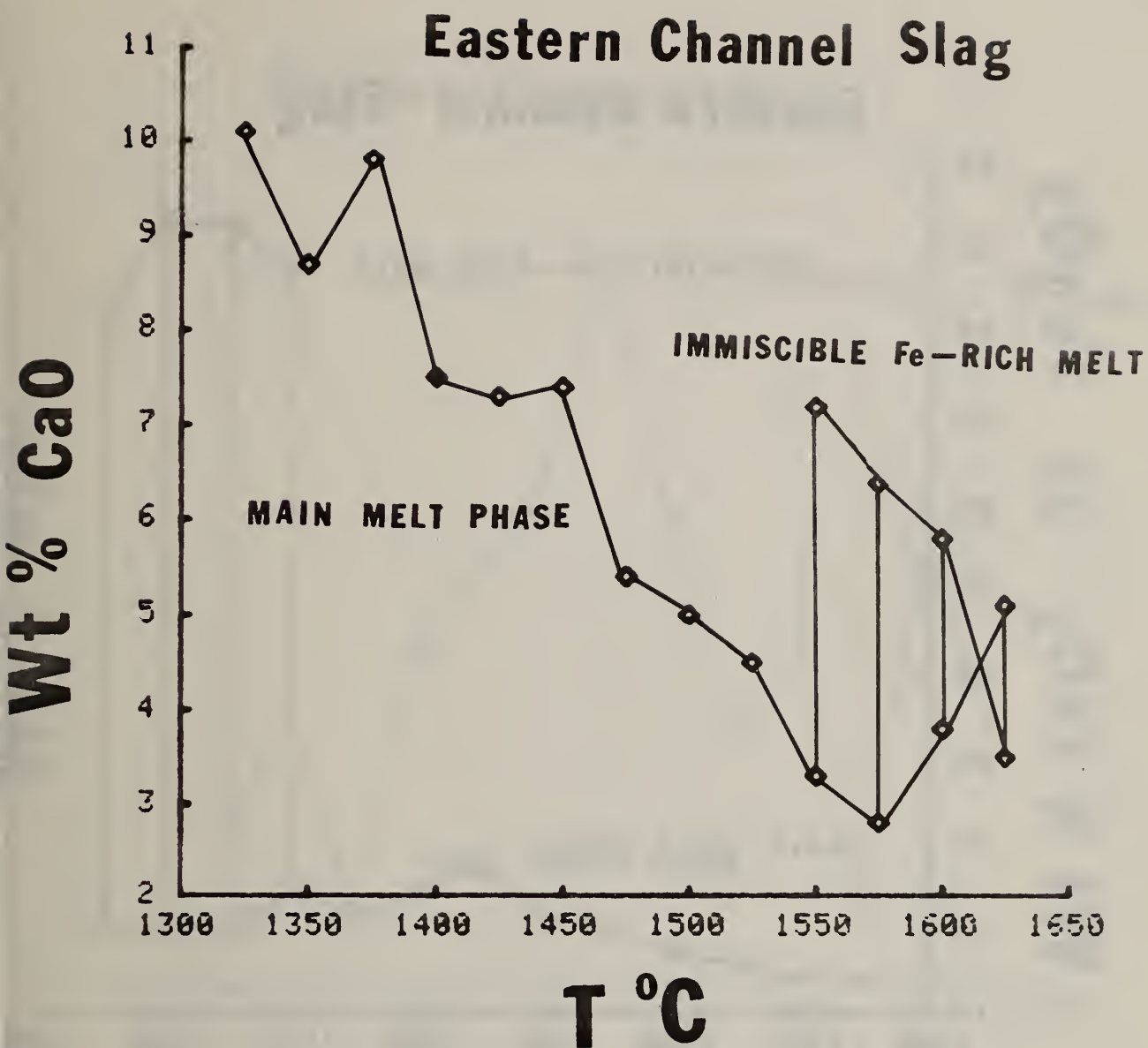


Figure 5. Semiquantitative analyses (I/I) of wt % SiO₂ as a function of T(°C) in res. slag phases for model "Eastern" channel slag composition.



6. Semiquantitative analyses (I/I) of wt % CaO as a function of T(°C) in residual slag phases for model "Eastern" channel slag composition.

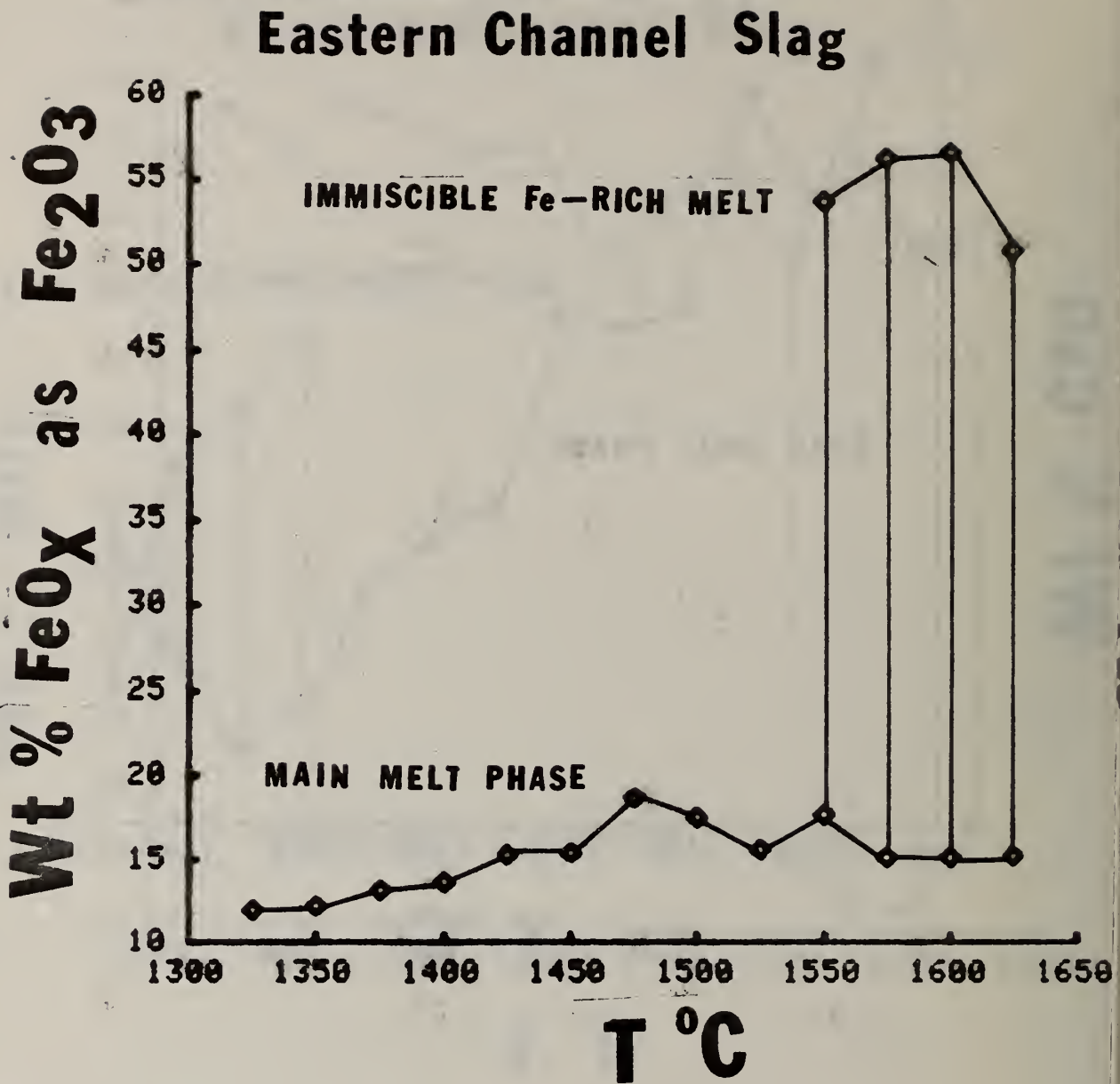


Figure 7. Semiquantitative analyses (I/I₀) of wt % FeO_x as Fe₂O₃ as a function of T(°C) in residual slag phases for model "Eastern" channel slag composition.

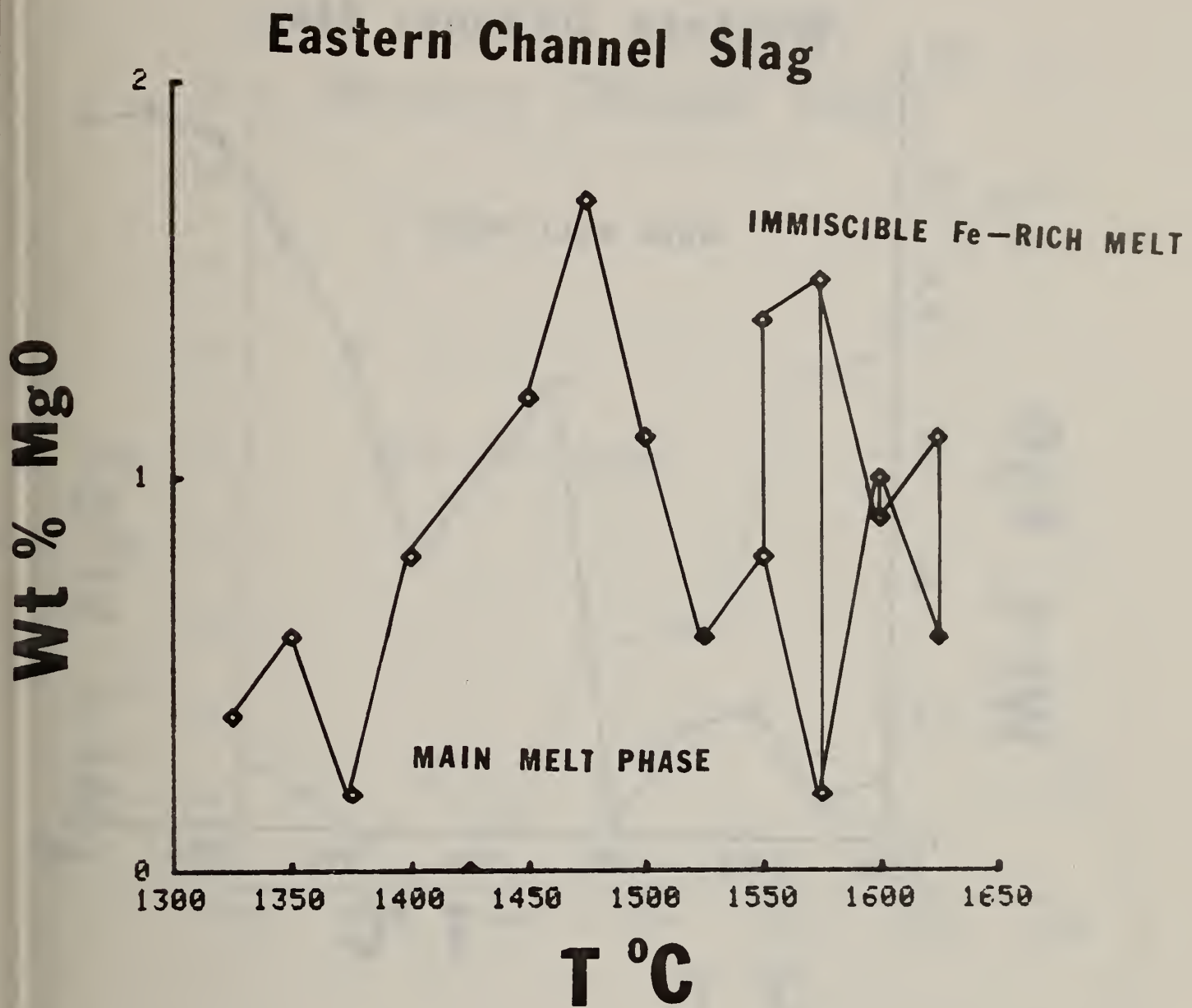


Figure 8. Semiquantitative analyses (I/I₀) of wt % MgO as a function of T(°C) in residual slag phases for model "Eastern" channel slag composition.

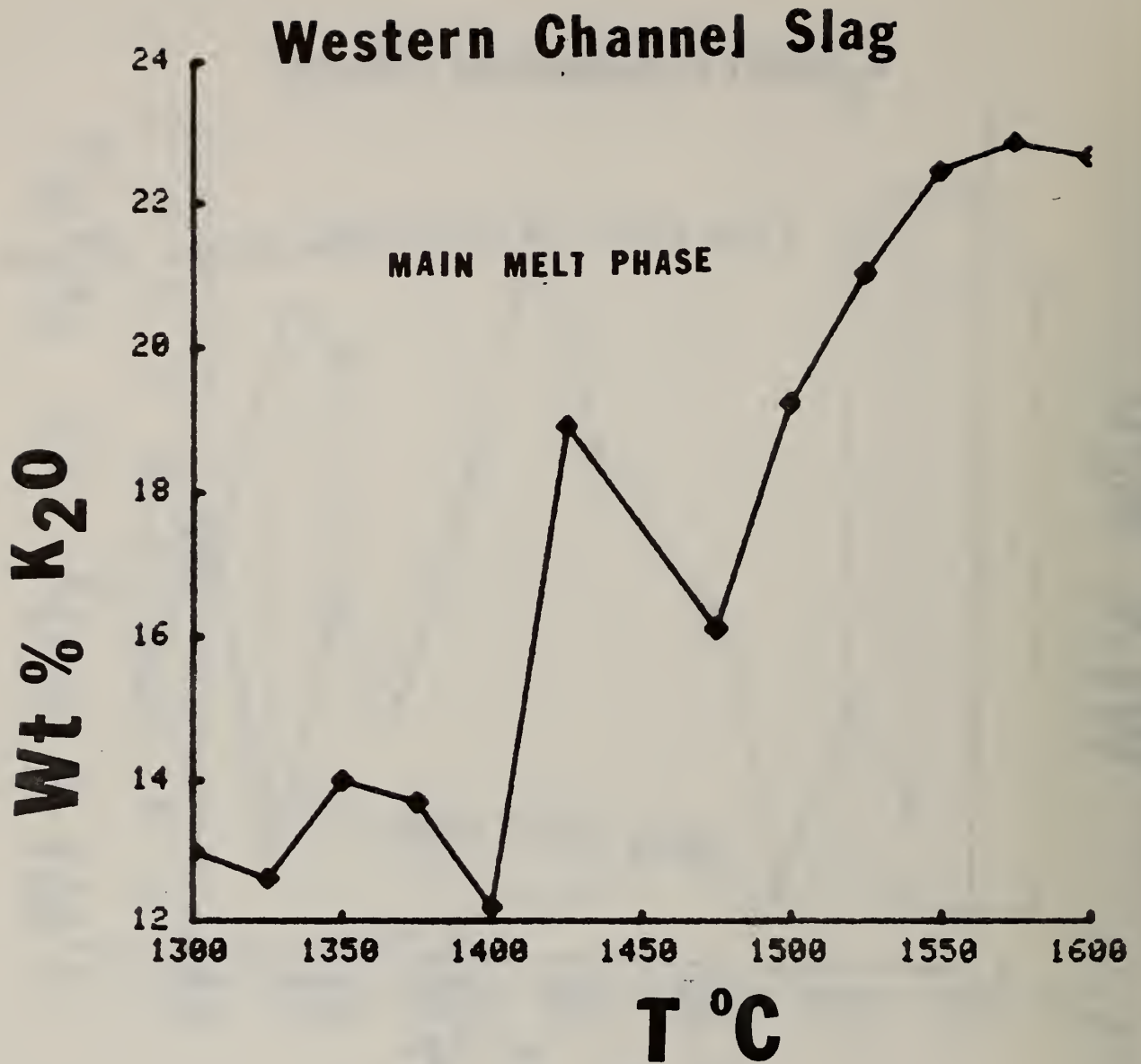


Figure 9. Semiquantitative analyses (I/I₀) of wt % K₂O as a function of T(°C) in residual slag phases for model "Western" channel slag composition.

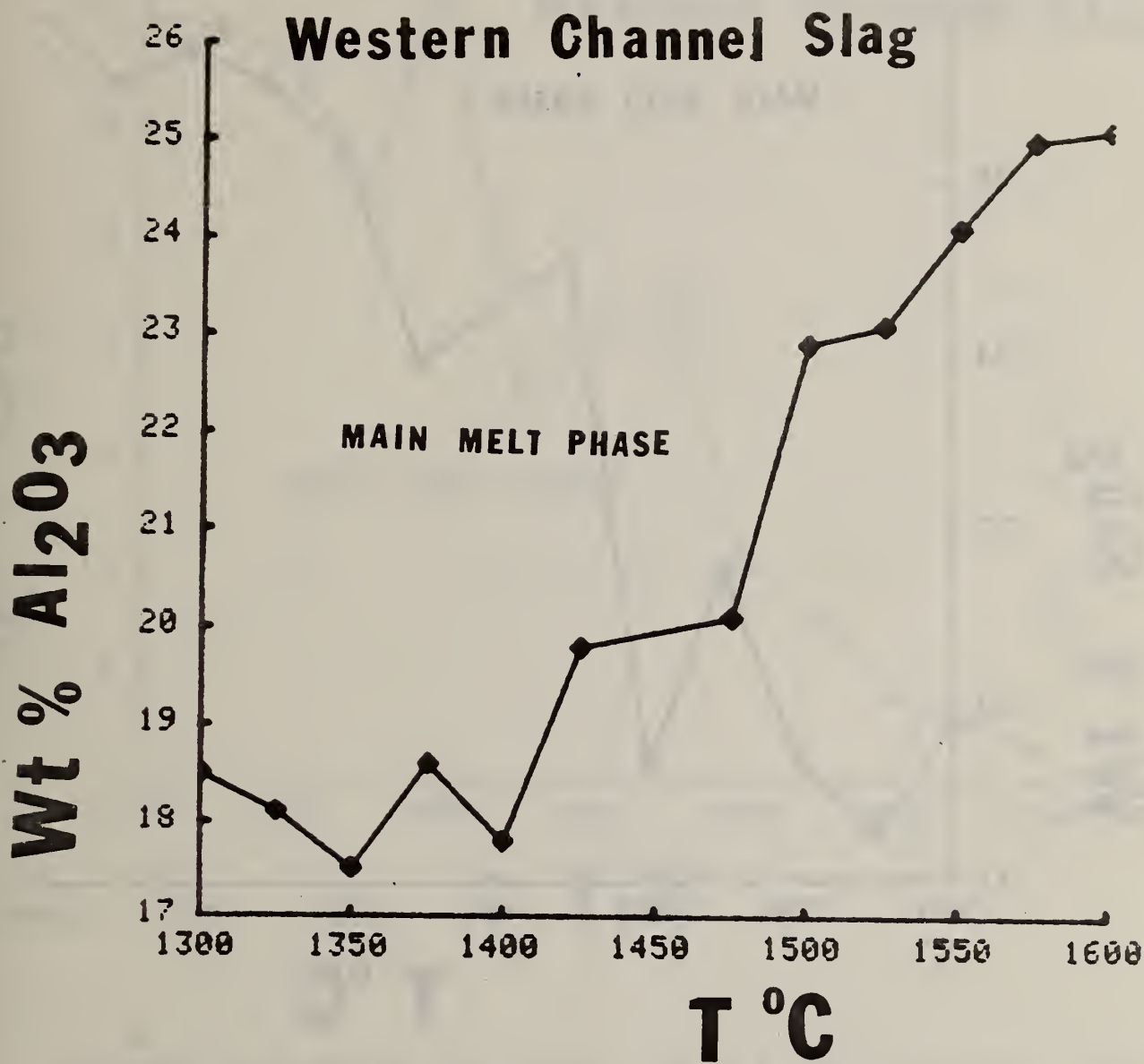


Figure 10. Semiquantitative analyses (I/I) of wt % Al₂O₃ as a function of T(°C) in residual slag phases for model "Western⁹" channel slag composition.

Western Channel Slag

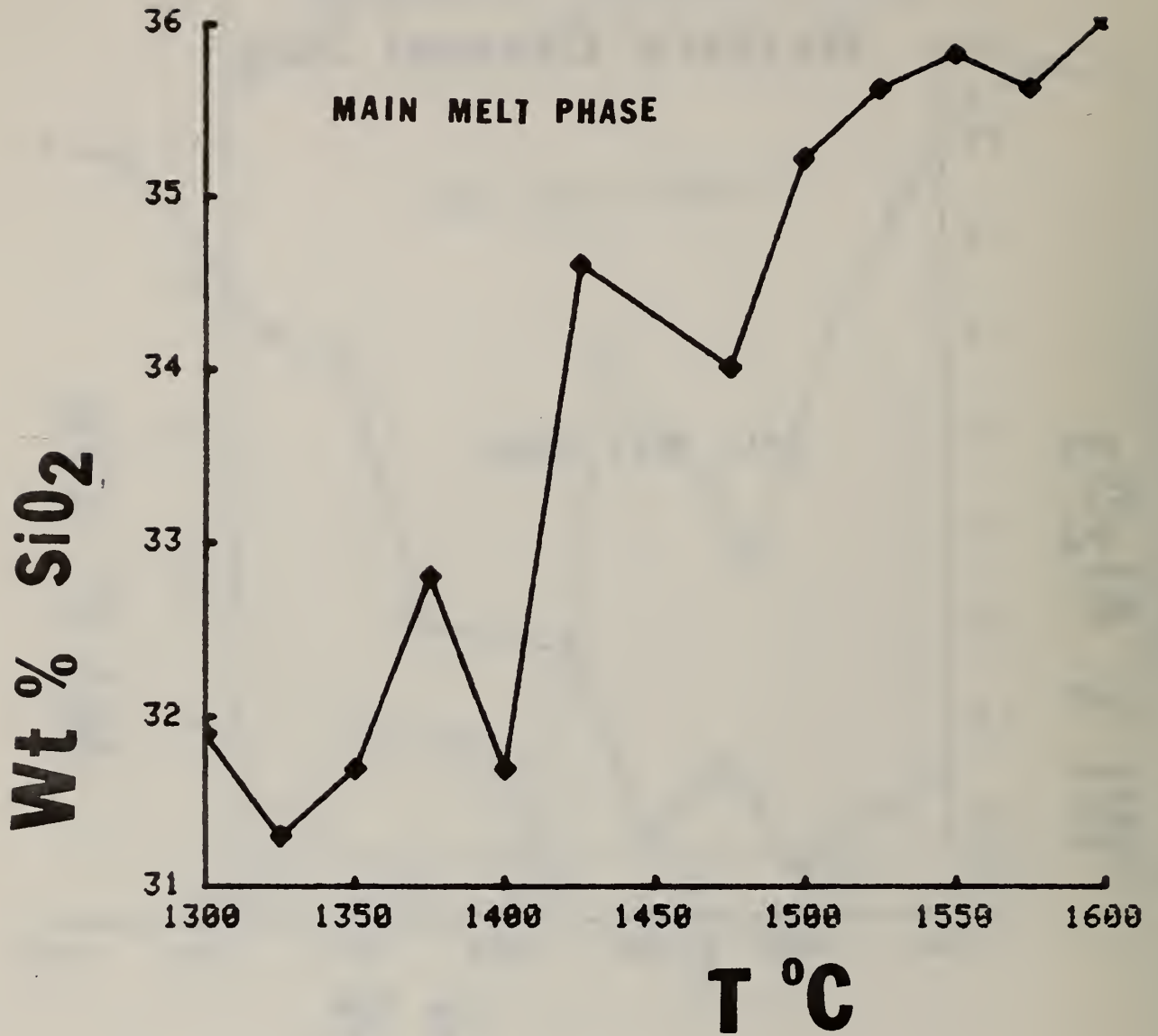


Figure 11. Semiquantitative analyses (I/I) of wt % SiO₂ as a function of T(°C) in res. slag phases for model "Western" channel slag₂ composition.

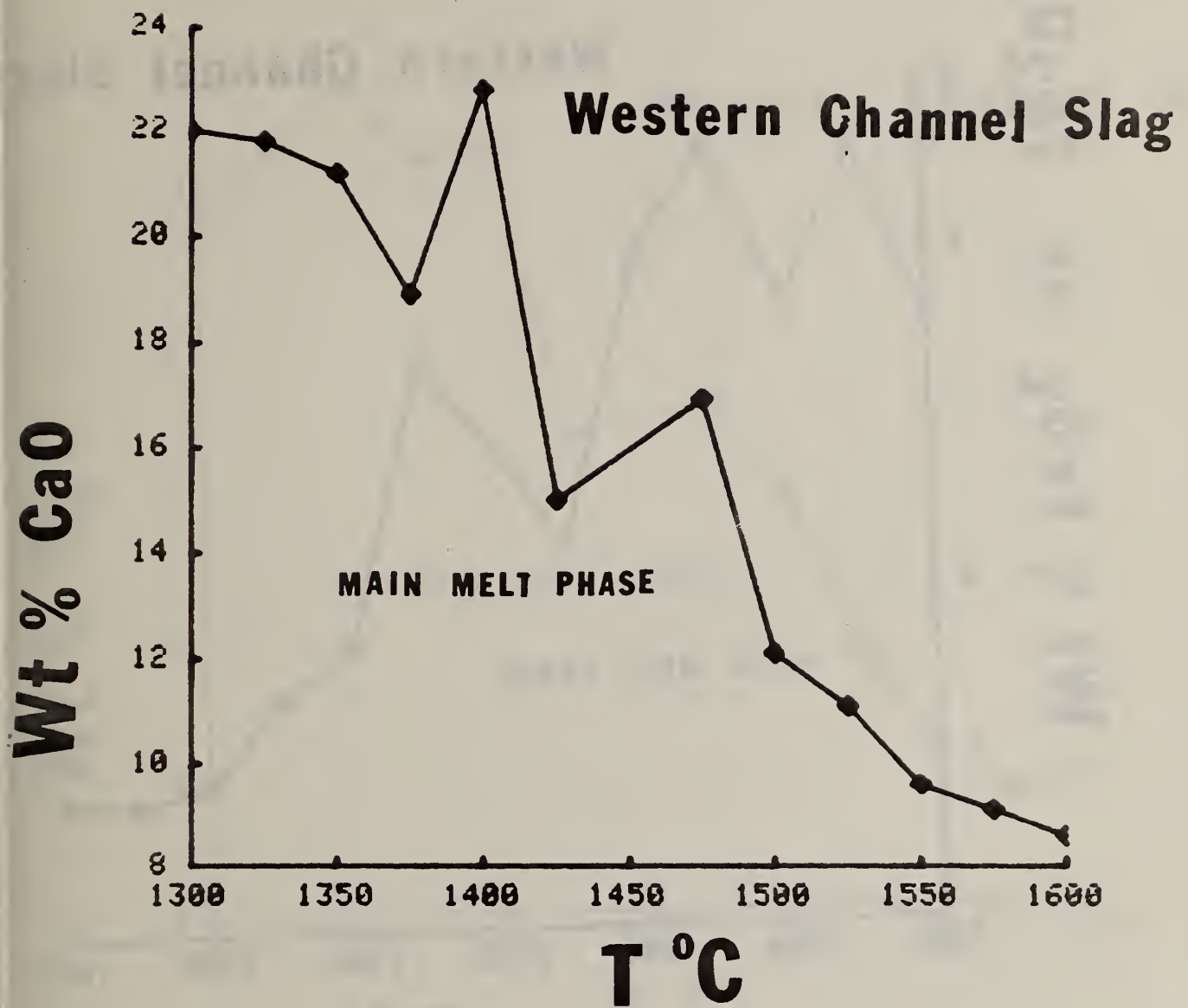


Figure 12. Semiquantitative analyses (I/I) of wt % CaO as a function of T(°C) in residual slag phases for model "Western" channel slag composition.

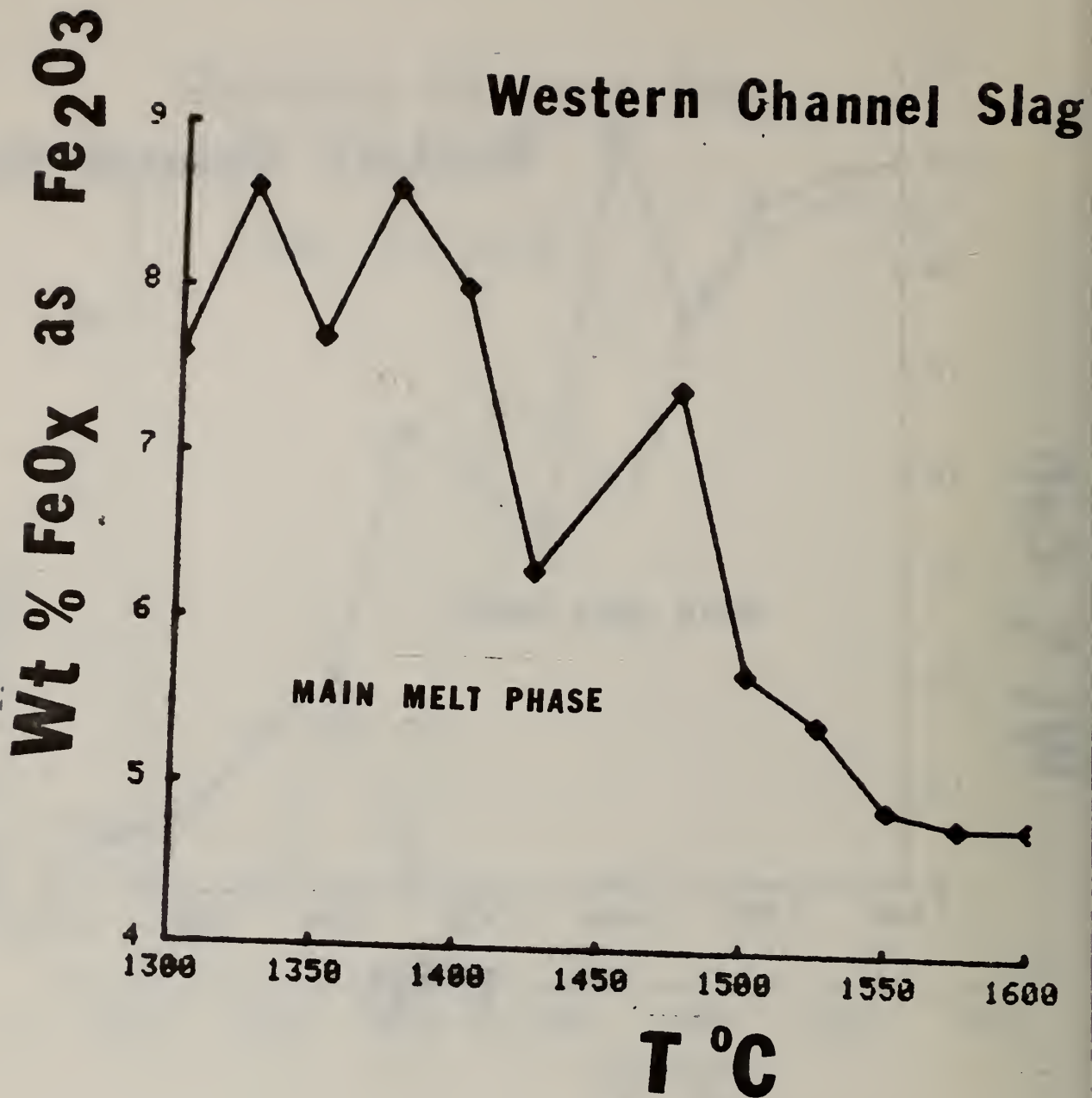


Figure 13. Semiquantitative analyses (I/I) of wt % FeO_x as Fe₂O₃ as a function of T(°C) in residual slag phases for model "Western" channel slag composition.

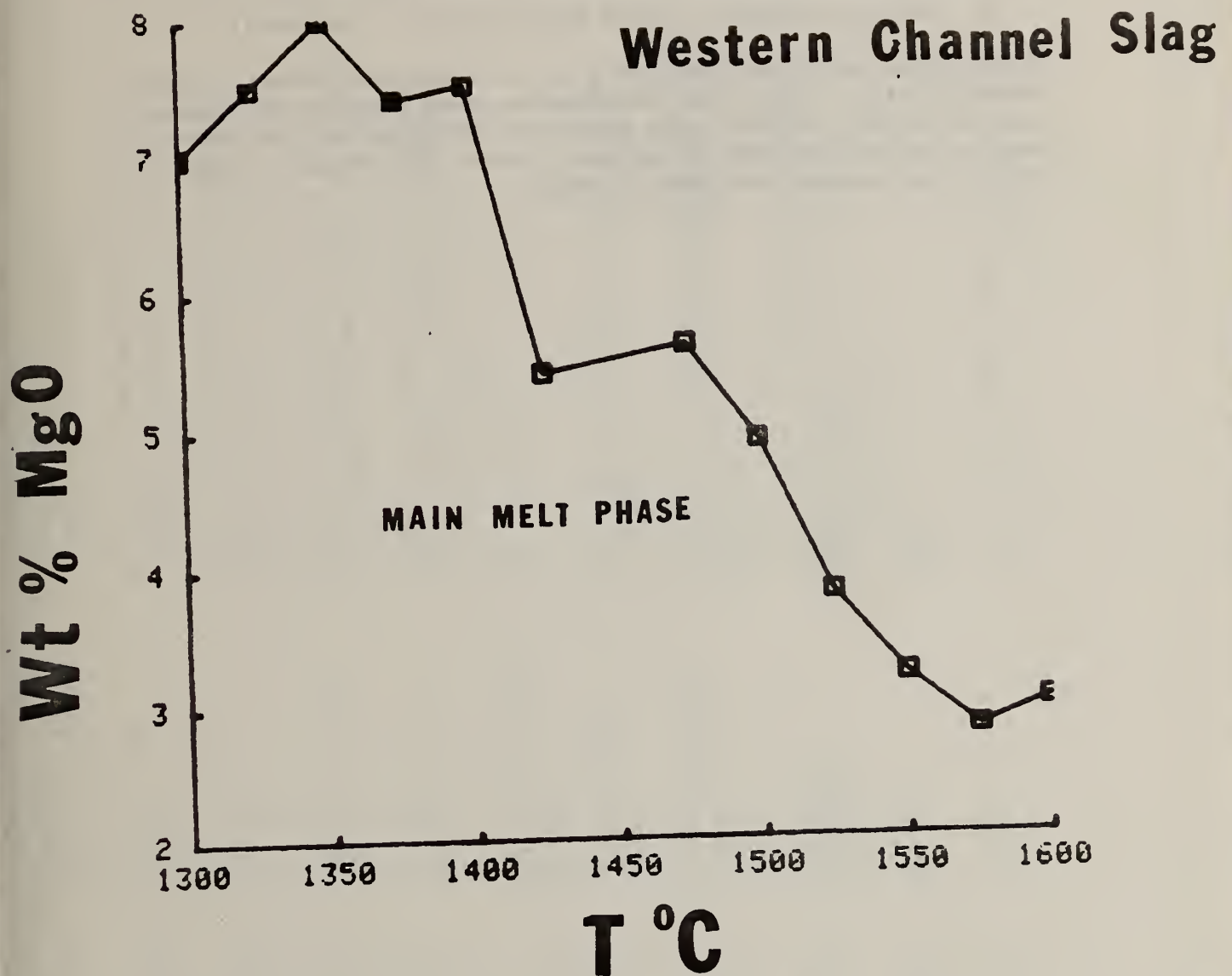


Figure 14. Semiquantitative analyses (I/I) of wt % MgO as a function of T(°C) in residual slag phases for model "Western" channel slag composition.

TASK K. MATERIALS TESTING AND CHARACTERIZATION

1. Structural Analysis of Powdered and Solid Ceramics

a. X-ray Diffraction of MHD Materials (C. L. McDaniel)

During this quarter we received about 50 materials (powders, dense ceramics, etc.), which were analyzed by x-ray diffraction methods. These materials include those developed at NBS as well as those sent to us by other MHD contractors. Data, transmitted to the appropriate source, are shown in Table 1.

Material	From	Description	Type Phase Present	Crystallinity
70LaCrO ₃ -30ZrO ₂ Cathode 1101 ²	Westinghouse U-02 Phase III	Molten like material; powder*	La ₂ Zr ₂ O ₇ pyrochlore + LaCrO ₃ perovskite solid solution	Medium to Good
LaCrO ₃ -LaAlO ₃ Cathode 1207	Westinghouse U-02 Phase III	Flowed crust; powder*	La(Cr,Al)O ₃ perovskite solid solution + La ₂ Zr ₂ O ₇ pyrochlore + cubic ZrO ₂	Medium to Good
LaCrO ₃ -LaAlO ₃ Cathode 1210-1211	Westinghouse U-02 Phase III	MgO insulator; powder*	MgO + La ₂ Zr ₂ O ₇ pyrochlore + MgAl ₂ O ₄ spinel + La(Cr,Al)O ₃ perovskite solid solution	Medium
LaCrO ₃ -LaAlO ₃ Cathode 1211	Westinghouse U-02 Phase III	Partially melted; powder*	La(Cr,Al)O ₃ perovskite solid solution + La ₂ Zr ₂ O ₇ pyrochlore + MgAl ₂ O ₄ spinel	Poor
70LaCrO ₃ -30ZrO ₂ Cathode 1526 ²	Westinghouse U-02 Phase III	Flowed crust; powder*	Cubic ZrO ₂ + La(Cr,Al)O ₃ perovskite solid solution + La ₂ Zr ₂ O ₇ pyrochlore + MgAl ₂ O ₄ spinel	Poor to Medium
70LaCrO ₃ -30ZrO ₂ Cathode 1529 ²	Westinghouse U-02 Phase III	Insulating wall; powder*	MgO + La(OH) ₃	Medium to Good
LaMg ₀₂ Cr ₉₈ O ₃ Cathode 1631	Westinghouse U-02 Phase III	Flowed crust; powder*	La(Cr,Al)O ₃ perovskite solid solution + La ₂ Zr ₂ O ₇ pyrochlore + cubic ZrO ₂	Medium
LaMg ₀₂ Cr ₉₈ O ₃ Cathode 1633	Westinghouse U-02 Phase III	Molten material; powder*	At least two "LaCrO ₃ " perovskite solid solutions + La ₂ Zr ₂ O ₇ pyrochlore + MgO + cubic ZrO ₂	Poor
LaMg ₀₂ Cr ₉₈ O ₃ Cathode 1634-1635	Westinghouse U-02 Phase III	Insulator (MgAl ₂ O ₄); powder*	La(Cr,Al)O ₃ perovskite solid solution + MgAl ₂ O ₄ spinel + cubic ZrO ₂ + K-La ₂ O ₃ ·11Al ₂ O ₃	Medium to Good
MgO Insulator wall	Westinghouse U-02 Phase III	powder*	MgO	Good
Upstream Insulator	Westinghouse U-02 Phase III	powder*	MgO + cubic ZrO ₂ + MgAl ₂ O ₄	Medium to Good

YCrO ₃ + MgO	Univ. Dayton	solid	YCrO ₃ solid solution	Medium
52CrO ₃ -48MgO	Westinghouse MC-AT 0301	solid	MgCr ₂ O ₄ + CrO ₃ + unknown perhaps CrO _x	Good
Cr ₂ O ₃	Westinghouse CO-AT 0101	solid	Cr ₂ O ₃	Very Good
98Cr ₂ O ₃ -2MgO	Westinghouse MC-AT 0701	solid	Cr ₂ O ₃ + MgCr ₂ O ₄	Good
MgCr ₂ O ₄	Westinghouse MC-AT 0101	solid	MgCr ₂ O ₄	Very Good
48Cr ₂ O ₃ -52MgO	Westinghouse MC-AT 0401	solid	MgCr ₂ O ₄	Very Good
56MgO-44Cr ₂ O ₃	Westinghouse MC-AT 0601	solid	MgCr ₂ O ₄ + MgO	Very Good
60MgO-40Cr ₂ O ₃	Westinghouse MC-AT 0501	solid	MgCr ₂ O ₄ + MgO	Good
Y (Mg .05 Cr .95)O ₃	Westinghouse YC-AT 0101	solid	YCrO ₃ solid solution + Y ₂ O ₃ + trace unknown (CrO _x)	Good
*Flow (Cathode side)** C-101	Westinghouse U-02 Phase III	powder*	Cubic ZrO ₂ + MgAl ₂ O ₄ + La ₂ Zr ₂ O ₇ pyrochlore + monoclinic ZrO ₂	Medium
Flow (cathode side)** C-201	Westinghouse U-02 Phase III	powder*	Monoclinic ZrO ₂ + cubic ZrO ₂ + K-β-Al ₂ O ₃ + K-β"-Al ₂ O ₃ (Mg) + Al ₂ O ₃ + MgAl ₂ O ₄	Medium
Flow (anode side)** A-202	Westinghouse U-02 Phase III	powder*	Monoclinic ZrO ₂ + cubic ZrO ₂ + K-β-Al ₂ O ₃ + MgO + Al ₂ O ₃ + MgAl ₂ O ₄	Medium
*Flow (anode side)** A-203	Westinghouse U-02 Phase III	powder*	K·La ₂ O ₃ ·11Al ₂ O ₃ + monoclinic ZrO ₂ + K-β-Al ₂ O ₃	Medium

Flow (Cathode side)**	Flow (anode side)**	Westinghouse U-02 Phase III	powder*	MgO + K ₂ CO ₃ · 1 1/2H ₂ O	Good
C-102-3	A-204-3	Westinghouse U-02 Phase III	powder*	Monoclinic ZrO ₂ + MgAl ₂ O ₄ + cubic ZrO ₂	Medium
	A-205	Westinghouse U-02 Phase III	powder*	Monoclinic ZrO ₂ + cubic ZrO ₂ + K-β-AL ₂ O ₃ + Al ₂ O ₃ + K-β''-AL ₂ O ₃ (Mg)	Medium
	C-103-2	Westinghouse U-02 Phase III	powder*	K·La ₂ O ₃ · 11Al ₂ O ₃ + MgAl ₂ O ₄ + monoclinic ZrO ₂ + cubic ZrO ₂	Poor to Medium
	A-206	Westinghouse U-02 Phase III	powder*	Cubic ZrO ₂ + monoclinic ZrO ₂ + K-β-AL ₂ O ₃ + K-β''-AL ₂ O ₃ (Mg)	Medium
	La .95Mg .05CrO ₃ Cathode 1420	Westinghouse U-02 Phase III	material near top; powder*	LaCrO ₃ solid solution + La(OH) ₃	Poor
	LaMg .02 .98O ₃ Cathode 1631	Westinghouse U-02 Phase III	material near top; powder*	LaCrO ₃ solid solution + La(OH) ₃	Good
	LaMg .02 .98O ₃ Cathode 1632	Westinghouse U-02 Phase III	material near top; powder*	La(OH) ₃ + LaCrO ₃ solid solution	Poor
	LaMg .02 .98O ₃ Cathode 1633	Westinghouse U-02 Phase III	material near top; powder*	LaCrO ₃ solid solution + La(OH) ₃	Medium
	LaMg .02 .98O ₃ Cathode 1631	Westinghouse U-02 Phase III	yellow material near bottom; powder*	La(OH) ₃ + K ₂ CrO ₄ + trace unknown	Good
	YCrO ₃ + MgO MS-8072	Trans-Tech	solid	YCrO ₃ solid solution + MgCr ₂ O ₄	Medium
	Y .98Ca .02CrO ₃ BI-1	Trans-Tech	powder	YCrO ₃ solid solution + Y ₂ O ₃	Medium
	Y .95Ca .05CrO ₃ BI-2	Trans-Tech	powder	YCrO ₃ solid solution + Y ₂ O ₃	Medium

Y _{0.90} Ca _{0.10} CrO ₃ BY-3	Trans-Tech	powder	YCrO ₃ solid solution + Y ₂ O ₃	Medium
Pt No. 2	AVCO	solid	Pt	Good
LaCrO ₃ No. 2	AVCO	solid	LaCrO ₃ + perhaps trace LaOOH	Medium
80Pt·20Fe	Goldsmith	powder	Pt solid solution	Poor
Y _{0.98} Ca _{0.02} CrO ₃ MS 8407	Trans-Tech	solid	YCrO ₃ solid solution	Medium
Y _{0.98} Ca _{0.02} CrO ₃ MS 8407	Trans-Tech	powder*	YCrO ₃ solid solution	Good
Y _{0.95} Ca _{0.05} CrO ₃ MS 8417	Trans-Tech	powder*	YCrO ₃ solid solution	Good
Y _{0.98} Ca _{0.02} CrO ₃ MS 8416	Trans-Tech	powder*	YCrO ₃ solid solution	Good
LaMg _{0.2} Al _{0.3} Cr _{0.75} O ₃ LC-AT1501A	Westinghouse	powder*	Two orthorhombic perovskite solid solutions	Good
LaMg _{0.2} Al _{0.3} Cr _{0.85} O ₃ LC-AT1501B	Westinghouse	powder*	Two orthorhombic perovskite solid solutions	Good
YCrO ₃ -MgO B-87	Univ. Dayton	powder*	YCrO ₃ solid solution + MgCr ₂ O ₄	Good
YCrO ₃ -MgO B-87A	Univ. Dayton	powder*	YCrO ₃ solid solution + MgCr ₂ O ₄	Good
YCrO ₃ -MgO B-87B	Univ. Dayton	powder*	YCrO ₃ solid solution + MgCr ₂ O ₄	Good
Pt No. 3	Goldsmith	powder	Pt	Very Good

*Received material as solid. Powder was prepared for X-ray analysis.

**These materials were from the flowing material at the junction of either the cathode and insulating wall, or the anode and insulating wall. For further information see Task K, section 3.3, this report.

2. Electrode Systems and Component Materials Test (W. R. Hosler, E. N. Farabaugh and T. Negas)

2.1 NBS/AVCO Slagging Test 2.

The six electrodes described in Quarterly Report, January-March 1978, page 38, have been sent to AERL in Everett, Mass. and testing will take place as soon as they can be accommodated in the MHD test channel there. There was a delay in the fabrication due to some difficulties in trying to incorporate the thermocouples just below the platinum cap during the spraying process. It was hoped that these thermocouples would give an indication of the cap temperature (a critical point in this electrode design). They have been eliminated. The specification on the cap thickness was decreased from 0.5 mm to 0.25 mm but the roll over on the upstream anode edge was specified at 0.5 mm or thicker. Several leaks at the water cooling tubes and passage plugs solder joints were detected and had to be repaired also.

While special arc plasma sprayable powder (nominally +10 to 40 μ) is used in fabricating these electrodes, the spraying efficiency is not good (<50%). Fortunately, most of the overspray and dusting powder can be retrieved.

2.2. U-02 Phase III, US-USSR Cooperative Program

The Phase III test carried out in Moscow from May 13-16, 1978, was described briefly in the last Quarterly Report (April-June, 1978 on page 57). Some findings in the post test analysis are given in section 3 of Task K of this report.

3. Test Analysis (Pre and Post Test Materials Characterization)

3.1 Analysis of AVCO Electrodes (T. Negas)

Representative anodes and cathodes from a recent long term test at AVCO were forwarded via DoE to NBS. The test apparently was discontinuous but 250 hr were accumulated mostly with slag. Cathodes were constructed from copper which was "capped" via a solder with a Cu/W metal composite. A nickel tab was soldered laterally to the Cu of each electrode. Boron nitride insulation was utilized between this Ni-tab and the Cu of the adjacent electrode. The cathode assembly provided a continuous, flat surface exposed to the plasma. Castable apparently was not utilized to promote "sticking" of slag and, indeed, little slag was noticeable on the post-test specimens. Anodes were constructed in a similar fashion. However, the copper was "capped" via a solder with oxidation resistant Pt-metal. The copper also was recessed at one extremity to accommodate a castable. After testing, the original castable was absent having interacted with slag. Figure 1 illustrates schematically the post-test condition of the electrodes.

Anodes and cathodes are in remarkably excellent post-test condition considering the rigors imposed by the AVCO test facility (this writer has not seen better). Both, however, display, in hand specimen, similar degradation and loss of metal. This recession is confined to the plasma side of regions originally encompassing (in cross section) the boron nitride/Ni-tab/Cu interfaces. The associated Pt and Cu/W "caps" as well as the recessed Cu areas remained relatively intact. It was speculated that electrochemical processes could account for the observed degradation and, indeed, a reasonable model probably can be formulated.

Electrode cross sections (polished) and untreated, perpendicularly disposed, metal surfaces exposed to slag/plasma were examined comprehensively by SEM/EDX methods. Categorical evidence indicative solely of electrochemically-induced corrosion, although not precluded, was not obtained. Gross features were either simple and obvious (e.g. melting) or so chemically complex that pinpointing of specific corrosion mechanisms and derivable conclusions cannot be fully justified. Major observations, nevertheless, are summarized below. Photographic evidence including elemental EDX analyses are on file and available.

1. Pt caps obviously were subjected to melting and developed a ridge-groove complex.
 - a. Slag constituents (Al, Si-rich plus K, Ca, Fe) are found frequently entrapped within the Pt and also form a discontinuous "scum" on the metal surface.
 - b. Detachment of the Pt was not serious, indeed, the underlying copper and solder is undercut to expose a leading ledge of beaded Pt metal.

1. The Cu/W cap sustained relatively little damage although the adjacent copper plus Ni-tab deteriorated. The surface of the Cu/W composite exposed to the plasma is chemically heterogeneous.
 - a. Melting is apparent in the direction of the Cu/solder/Ni/boron nitride sequence (area 1, Figure 1). A vesicular structure has developed in this region. The skeletal framework or matrix of this structure is beaded and Cu-rich (oxygen and sulfur plus traces of W, K, and Ca also are detected). This matrix encloses recessed, nearly rounded regions enriched in Cu plus W (O, S, K, Ca, and Ni also detectable). Frequent, irregularly-shaped "blobs" protrude from the matrix. These are Cu-rich with traces of Al, Si, S, and Fe. Others are Si-rich plus Na, Mg, Al, S, K, Ca, Fe, and Cu.
 - b. The Cu/W surface in the direction away (area 2, Figure 1) from the features noted above apparently is overlain by a thin "slag" veneer in which two types of chemical partitioning dominate,
 1. globules of Fe-rich material containing variable amounts of Al, Si, W, K, Ca, S, Ti, and Cu, and
 2. Cu/W-rich material containing Al, Si, S, K, Ca, and Fe.

2. Copper and nickel, as expected, are concentrated within "slag" adjacent to these construction materials at the insulator gap. Zinc from the solder also is evident.

a. Copper appears to be partitioned between, at least, two types of porous material,

1. a material rich in Al, Si, K, Ca, Ti, and Fe ("slag"), and

2. a K, S-rich phase with lesser Al, Si, and Fe contents.

b. Sulfur associated with K and Cu is frequently detected toward the cooler end of the copper cup (previously containing castable) and immediately adjacent to exposed Ni/Cu construction materials.

c. Nickel is associated with "slag" adjacent to the tab but not with a K, S-rich material.

3. The exposed, remaining surface of the Ni-tab (area 1, Figure 1) (not well bonded to the overlying slag) yields strong oxygen signals suggesting oxidation; Al and Si frequently are associated with Ni and O. A Ca-rich scum adheres to the Ni-tab surface adjacent to the boron nitride (area 3, Figure 1).

2. In cross section, "slag" is practically absent. Sulfur, K-rich materials are not observed. Potassium, however, has penetrated the Ni/solder/Cu region to nearly its lowermost extent.

3. The exposed Ni-tab surface (area 3, Figure 1) contains,

a. Cu/W rubble often associated with traces of Ni, Fe, Ca, and K,

b. particles of slag (Al, Si, K, Ca, Ti, Fe) containing Ni and Cu, and

c. material containing only Ni plus phosphorus.

4. Exposed Cu surfaces (area 2, Figure 1) detached from "slag" and adjacent to the Ni-tab and Pt cap are spongy to vesicular in nature. Frequent chemical associations include,
- a. Cu, Al, Si,
 - b. Cu, Fe,
 - c. Cu, Pt,
 - d. Cu, Si, K, Fe,
 - e. Cu, K, S, as noted in the adjacent slag, and
 - f. oxygen always is detectable.

4. The exposed Cu surface (area 4, Figure 1) adjacent to the Ni-tab and Cu/W cap is extremely heterogeneous chemically. K, Ca, Fe associations with Cu are frequent. Oxygen and even carbon are frequently detected.

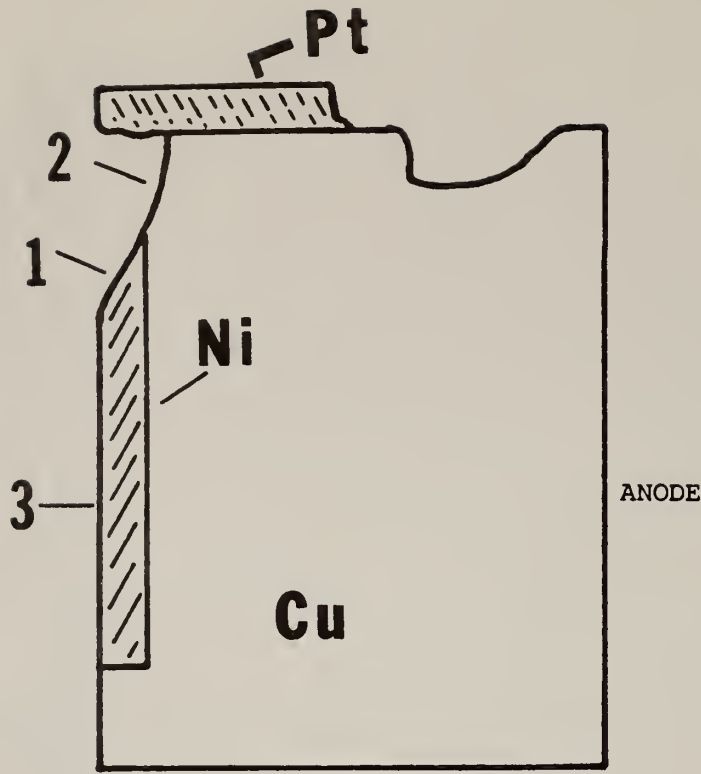
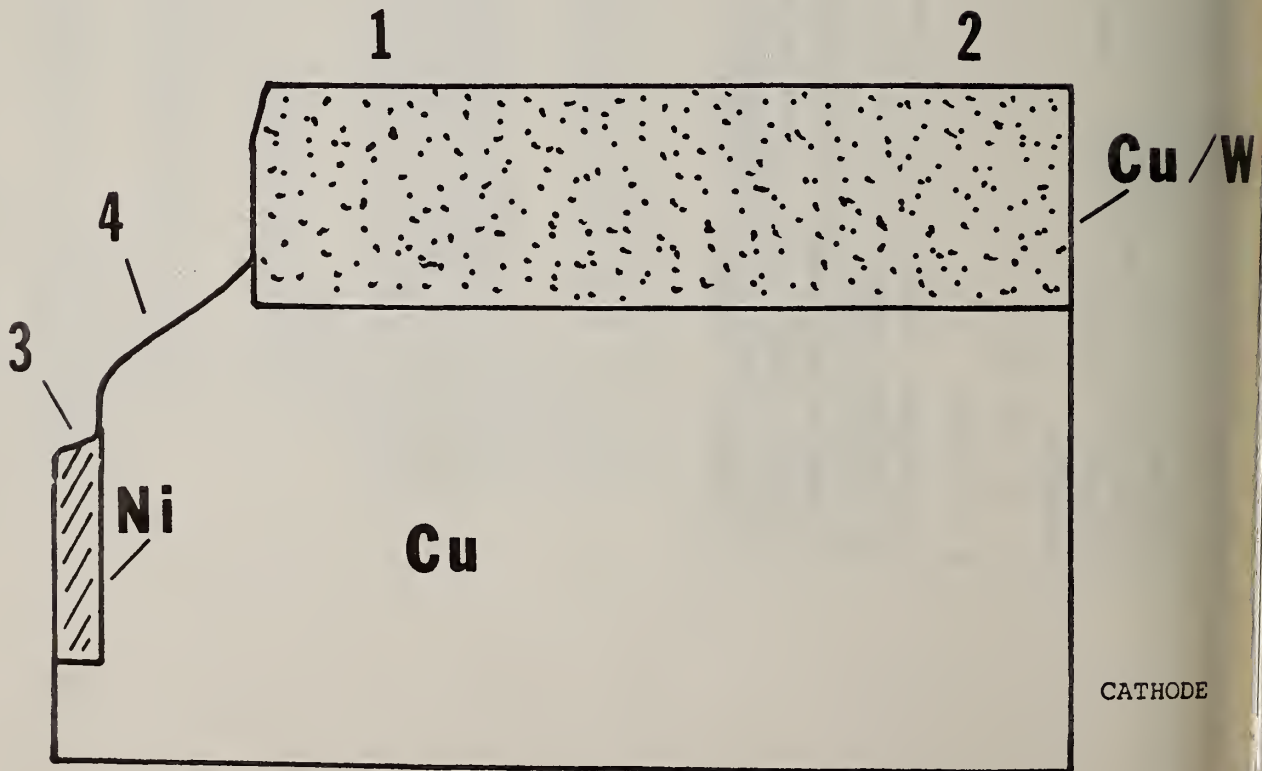


Figure 1. Post-test condition of AVCO electrodes.



U-25, RM Channel Deposits (T. Negas, C. L. McDaniel)

S. J. Schneider, during his recent visit in Moscow, obtained two types of "deposits" derived from the U-25, RM channel. Figure 2A,B illustrates material (designated as Z) obtained from near the generator inlet while Figure 3A,B,C shows a material (designated as C) taken from near the channel outlet. Material C apparently was located at the intersection of the side and upper generator walls.

Specimens from the above materials were collected for x-ray diffraction analyses. Material Z consists of monoclinic plus cubic variants of zirconia. The discolored, wall side portion (Figure 2A) is dominated by the cubic phase while the plasma side material (Figure 2B) consists of nearly equal amounts of both variants. Specimens will be analyzed by EDX to deduce what oxides were utilized to achieve at least partial stabilization of the monoclinic ZrO_2 . This, possibly, will then aid in determining whether the material has origins from the generator combustor sections.

Material C is much more complex. The main bulk with a pinkish discoloration (note Figure 3) consists of unaltered Al_2O_3 plus $AlPO_4$. The pinkish coloration is due to chromium as determined by EDX analyses (Si, Fe, Ni and even Ag were noted as frequent impurities). The phase assemblage including the presence of chromium strongly suggests that material C is a chrome-aluminum phosphate bonded, aluminum oxide-based castable or cement. If considered necessary, microstructure and microchemistry also will be pursued. The plasma side of material C is frequently intermixed and overlain by rivulets of white to buff material (note Figure 3A,C). These consist of zirconia (monoclinic plus cubic) admixed with alumina and probably represent a phase once fluid derived from upstream (combustor?) materials. Part of the interior and wall side of material C (Figure 3B) are characterized by corrosion products having green to brown discoloration. These products consist predominately of K- β alumina. However, other corrosion products are present as indicated by distinct hydration and swelling at room temperature. Associated x-ray patterns yield weak, broad, maxima (not seed) which cannot be interpreted unambiguously.

[The text in this section is extremely faint and illegible. It appears to be a list of items or a series of paragraphs, possibly containing names, dates, and descriptions. The text is too blurry to transcribe accurately.]

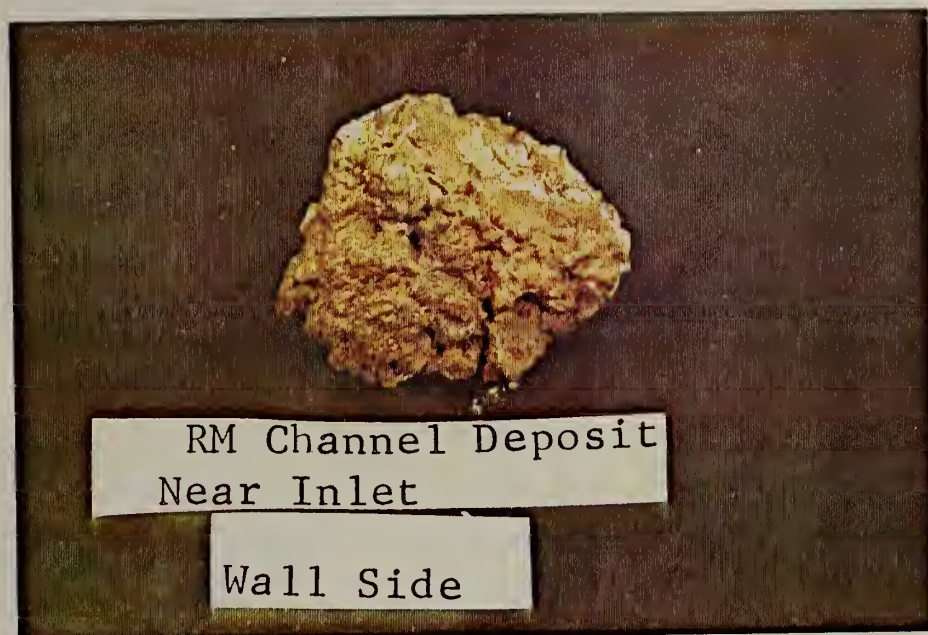


Figure 2A. U-25, RM channel Deposit.

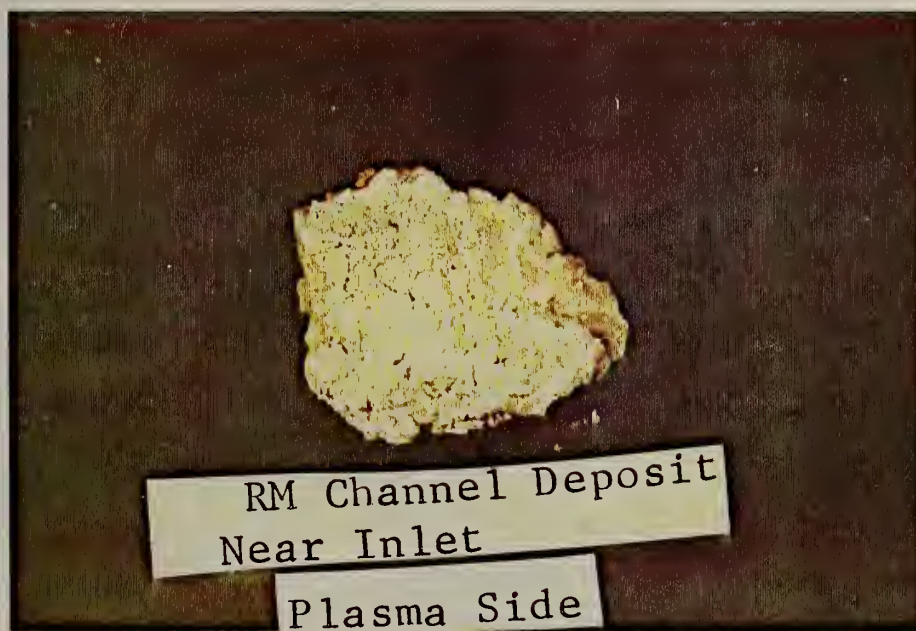
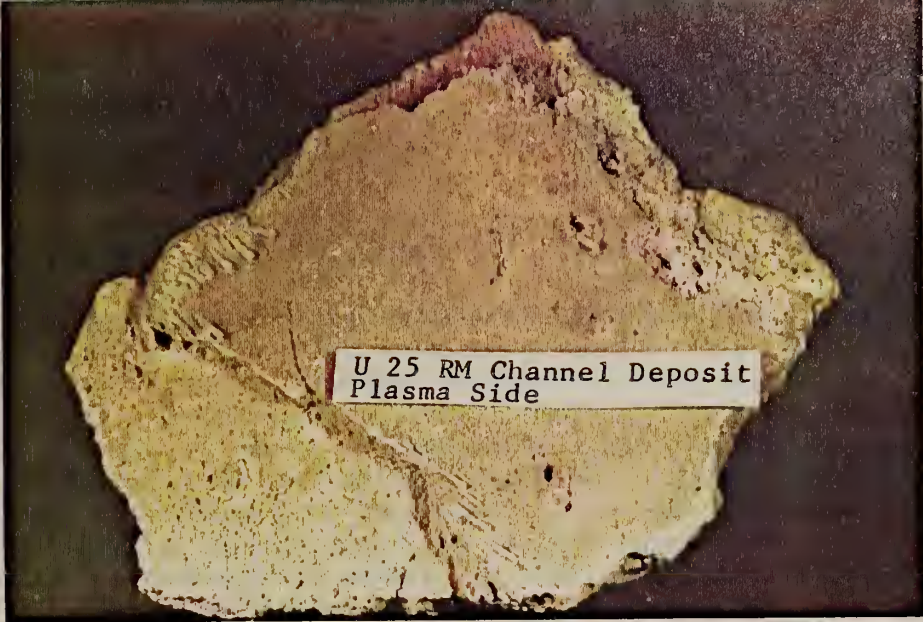


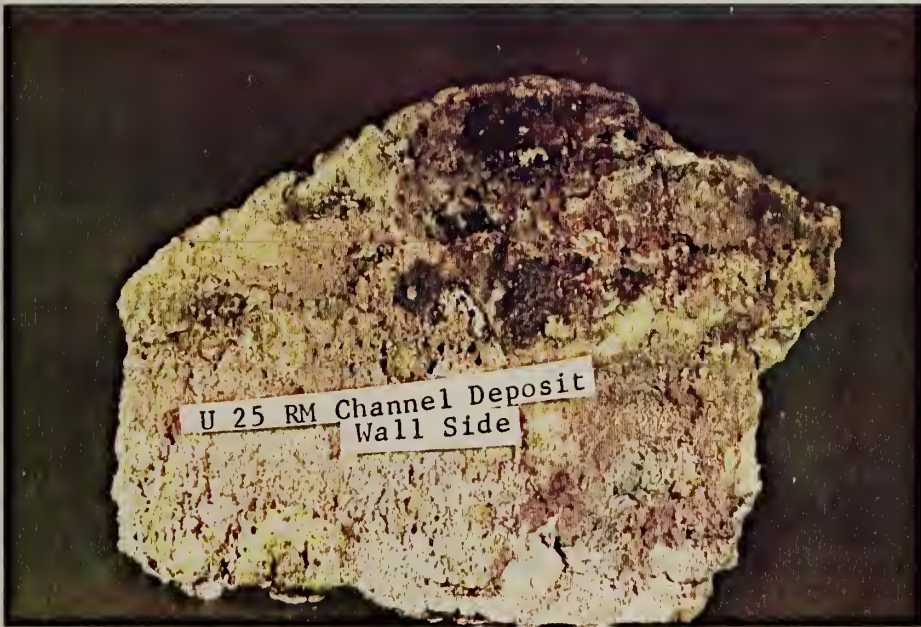
Figure 2B. U-25, RM Channel Deposit.

Figure 3A.



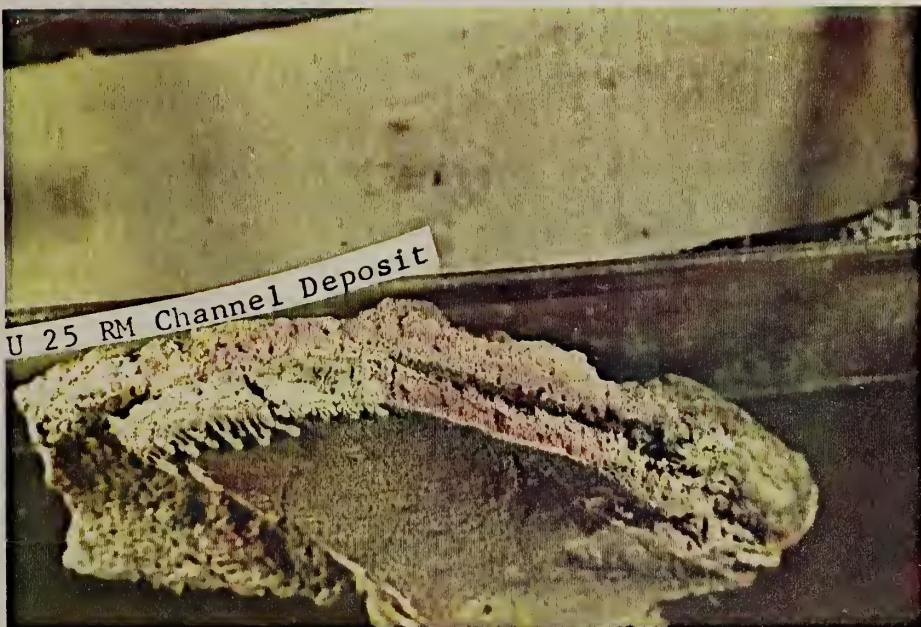
U 25 RM Channel Deposit
Plasma Side

Figure 3B.



U 25 RM Channel Deposit
Wall Side

Figure 3C.



U 25 RM Channel Deposit

3.3 U-02, Phase III, Westinghouse Test (W. R. Hosler, T. Negas, L. P. Cook, E. N. Farabaugh, C. L. McDaniel, A. Perloff)

During this reporting period post-test analytical data derived from the U-02, Phase III module, are limited mostly to x-ray diffraction work and radiography. Portions of the USSR, MgO-based insulating wall adjacent to the electrode walls also were received and subjected to x-ray analysis. Power supply problems for over one month have precluded additional work utilizing SEM/EDX methods. A final report to DoE and Westinghouse is scheduled for the end of October 1978, although our preliminary data have been discussed with Westinghouse personnel. The completed report (or salient results and conclusions) will be given in the next quarterly report.

During the course of the Phase III test a flowing layer of material of relatively high viscosity formed near the perpendicular junction of the U.S. electrode walls and the USSR insulating walls. This layer was discovered after cool down. During the run a steady decrease in the effectiveness of the interelectrode insulation was noted and post test observation of this fluid layer led to speculation that it might have contributed to the insulation degradation observed. Figures 4 and 5 show the electrical conductivity of an upstream and downstream sample of this flowing layer up to a temperature of about 1550 °C.

The results of the conductivity measurements shown in Figures 4 and 5 do not conclusively prove that this layer was solely responsible for the interelectrode insulation degradation.

X-ray diffraction data (Task K - section 1, this report) indicated a large amount of β -alumina present in this material. The origin of the alumina is not know. The foreign deposit was most heavy on the anode side and was beige in color while the lighter deposit on the cathode was partially pink probably due to the presence of chromium.

4. Materials Development and Analysis

4.1 YCrO₃-Based Ceramics (T. Negas, W. R. Hosler)

During this quarter several runs were conducted to prepare high density ceramic bars based on YCrO₃. Using precipitated and precalcined powders prepared at Trans-Tech Inc. ingots were thermally sintered at 1750-1760°C (6-8 hr) in a forming gas environment. Better than 95% of theoretical density ultimately was obtained for Y_{0.98}Mg_{0.02}CrO₃ and members within the series Y_{1-x}Ca_xCrO₃, $x \leq 0.05$. We are experiencing some difficulty with the $x = 0.10$ composition. This possibly can be traced back to the chemistry of the initial precalcined powder.

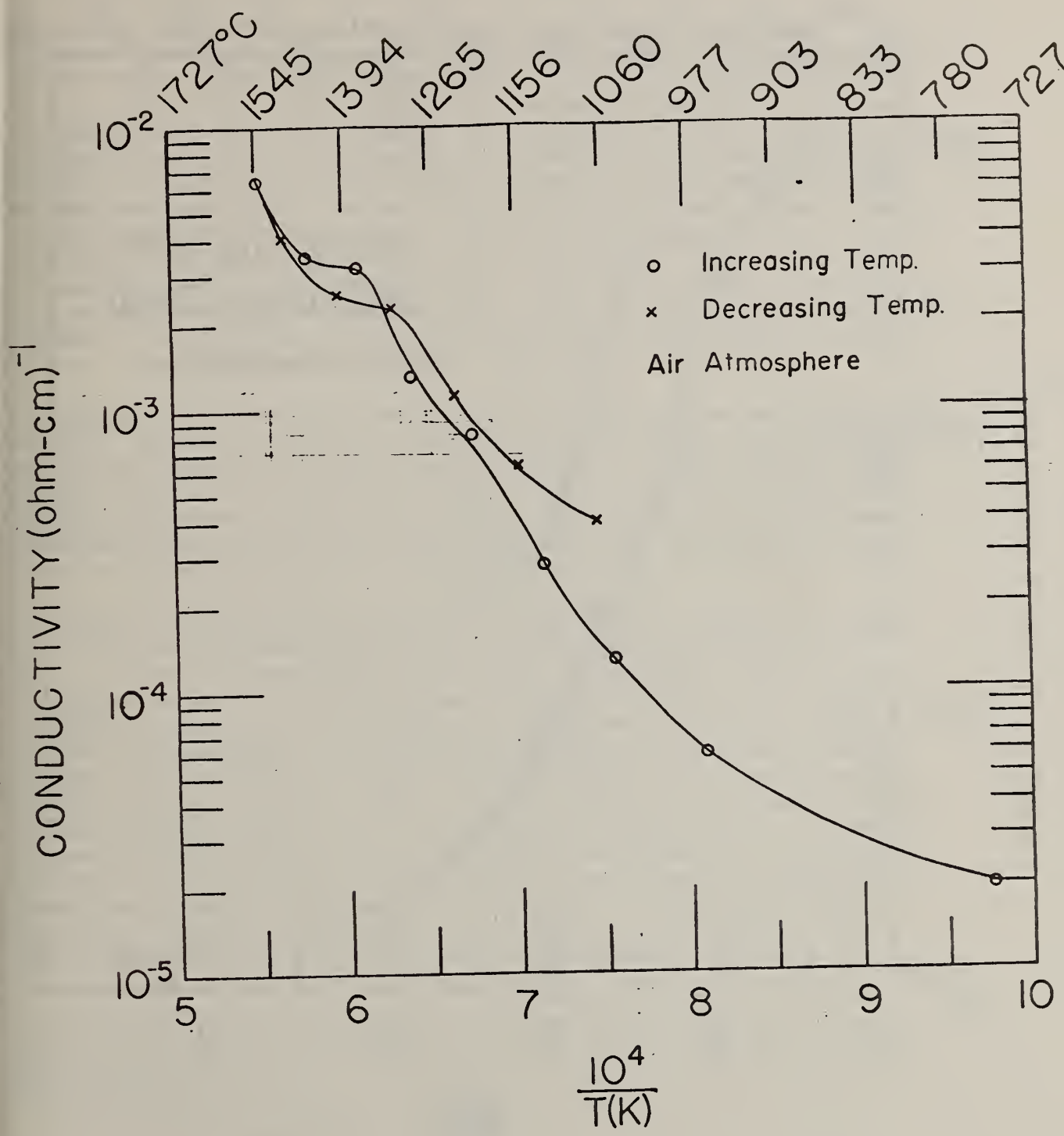


Figure 4.

Electrical conductivity as a function of temperature of the ceramic deposit on the insulating wall of U-02 (Phase III). This sample taken from upstream portion near anodes 2209 and 2213. (BNW M 129C)

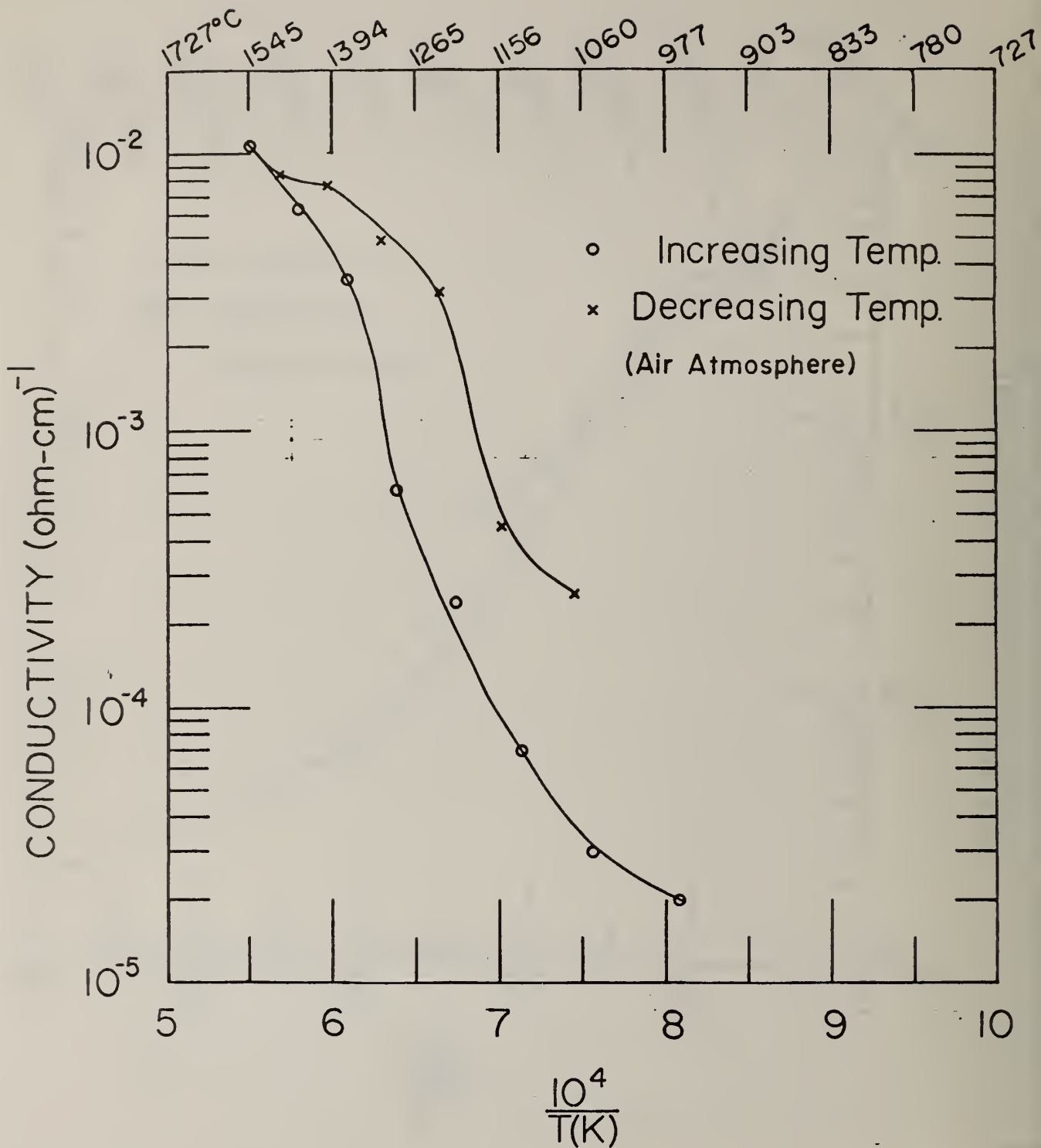


Figure 5.

Electrical conductivity as a function of temperature of ceramic deposit on the insulating wall of U-02 (Phase III). This sample taken from downstream portion near anode electrodes.

TASK L. ASSESSMENT OF STEAM PLANT COMPONENTS

1. Laboratory Hot Corrosion Screening Program (J. Smit)

One of the initial goals of this screening program was to develop procedures for detecting corrosion in its early stages. With appropriate metallographic techniques, SEM-EDX analysis, using a modified instrument capable of detecting light elements such as oxygen, appears to provide this capability. To date incipient corrosion has been detected in specimens that have been exposed to a hostile environment in our burner rig for relatively short times, test durations of about 4 hours (see Task L in the quarterly report for the period April-June 1978, "Development, Testing and Evaluation of MHD Materials"). In these short duration tests, if corrosion is detected, the suitability of the material for use in downstream components is questionable. If, however, no corrosion is detected, the converse does not necessarily apply. One can only say that the material showed no signs of corrosion for the time interval of the test. It then becomes necessary to test for longer intervals.

At present all our gas flows and cooling air flows are manually controlled. Regulator valves are trimmed by hand to maintain the hot zone temperature and specimen temperature at the required levels. Partly because of this and partly because of current gas supply limitations the rig cannot be operated unattended, this in turn limits test duration. To provide for unattended operation and hence long duration tests, when required, our rig is being rebuilt along the following lines.

A modified two gas blender-controller connected to the oxygen and propane lines and interfaced with a thermocouple output amplifier will be used to control automatically the hot zone temperature. The specimen temperature will be controlled automatically by a modified mass flow controller on the cooling air line and interfaced with another thermocouple output amplifier. The propane and oxygen supplies are being expanded from the single cylinder units now used. A six station manifold with supply and check valves is being obtained for the oxygen supply and a two station manifold also with supply and check valves is being acquired for the propane supply. With these manifolds and this valving, sufficient gas can be kept on hand to permit unlimited time duration runs. The automatic temperature control units will allow unattended operation. With the improved rig, those materials that survive the initial screening can be further tested to determine the effects of long time exposure.

Currently specimens of AISI 1015 steel, 310, 316 and 446 stainless steel are being evaluated. These materials have been exposed under the following conditions:

- a. Hot zone temperature 1330°C
- b. Specimen temperature 550°C
- c. Total test time 4 hrs.
- d. K_2SO_4 Flow rate 10 gm/min.

e. K_2SO_4 Flow time 30 min.

Metallographic specimens have been prepared from these pieces and are now being analyzed.

2. Material Assessment (J. R. Cuthill and D. J. Kahan)

A follow-up on the "800" alloys

INCO alloys 800 and 800H with the following respective nominal compositions:

	<u>Cr</u>	<u>Ni</u>	<u>Fe</u>	<u>Al</u>	<u>Ti</u>	<u>C</u>
800	21	32.5	46	0.38	.38	.05
800H	21	32.5	46	0.38	.38	.1

have been included in previous reports in the list of Selected Wrought Alloys (see for instance the quarterly report for the period ending Dec. 31, 1977) as alloys to be included in simulated performance testing. The "800" alloys, including the 801 variation with increased titanium to increase corrosion resistance to sulfur dioxide and stress corrosion, and 800H and 802 with increased carbon to develop carbide precipitation for maximum strength, respectively, have become widely used for many components of power plants both in the U.S. and in Europe (Ref. 1). Applications of 800 alloys in fossil-fuel fired power plants include steam superheater heat exchanger tubing and economiser and sulfur dioxide recovery units because of their generally all around superior properties, including: -

1. Very good high-temperature creep strength.
2. Good resistance to H_2S attack under certain conditions*. Resistance to H_2S attack twice that of 310 stainless steel. (see for instance previous quarterly report for period ending June 30, 1978.)
3. Good resistance to high-temperature oxidation, carburization, and hot corrosion.
4. Good resistance to stress corrosion cracking.
5. Good cold forming and weldability.

The specific alloy modifications alluded to previously are as follows: -

<u>Alloy</u>	<u>Modification</u>	<u>Application</u>
801	twice Ti content of "800" to optimize resistance to stress-cracking	heat exchangers for SO_2 recovery and hi-temp. steam
800H and 802	twice and 7 times C content of "800", respectively, to optimize high-temp. strength	hi-temp. steam heat exchanger tubing

*See "Limitations" for further details.

The relative cyclic high temperature oxidation resistance, resistance to scaling, of these alloys in air in respect to 304 and 309 stainless is shown in Figure 1 from "Incoloy Alloys" (Ref. 2), which is a good source for physical and mechanical properties. The relative allowable tensile stress for alloy 800 in respect to other commonly used alloys for power plant components, based on the ASME Boiler Code, is shown in Figure 2 from a review by Mesko (Ref. 3).

Papers at the Petten Conference, which was cited previously (Ref. 1), in addition to discussing applications of alloy 800 and its variations, also discussed the metallurgy and the limitations which one must be cognizant of in using these alloys. The principal limitations discussed can be summarized as follows: -

Limitations on Using Alloy 800

1. Incoloy 800 alloys are prone to the precipitation of sigma phase accompanied by sharp loss in ductility after long periods of service (30,000 to 40,000 hours) in the 600 - 750 °C range (Ref. 4).
2. Boron - containing coatings or boron in any form should not be applied to the 800 alloys because of its detrimental effect on welding properties (Ref. 4).
3. Perkins reports (Ref. 5) that alloy 800 can be used in a wide range of gas compositions containing a few ppm to 100% H₂S without significant attack, at temperatures below 1000 °F (583 °C). Excessive rates of attack are likely to occur above that temperature with 1% or more of H₂S in the gas. In an oxidizing atmosphere a reasonable life expectancy should be obtained at operating temperature up to 1200 °F (650 °C) unless CaO, (or presumably other alkali or alkaline earth oxides) are present in the gas which react to form sulfates that are molten on the alloy surface, resulting in hot corrosion and accelerated attack.

References

1. M. A. Cordani, Existing and Potential Applications for Alloy 800, Proceedings of the Petten International Conference on Alloy 800, held March 14-16, 1978, Petten, The Netherlands, North-Holland Publishing Co., Amsterdam (in press).
2. "Incoloy Alloys", published by Huntington Alloy Products Division of INCO, Huntington, WV 25720.
3. J. E. Mesko, Materials for Direct Combustion Fluidized - Bed Steam Generators, Metal Progress, 112, p. 30, July 1977.
4. J. Orr, A Review of the Structural Characteristics of Alloy 800, Proceedings of the Petten International Conference on Alloy 800, *ibid.*
5. R. A. Perkins, High Temperature Gaseous Corrosion of Incoloy 800 in Sulphidizing Environments, *ibid.*

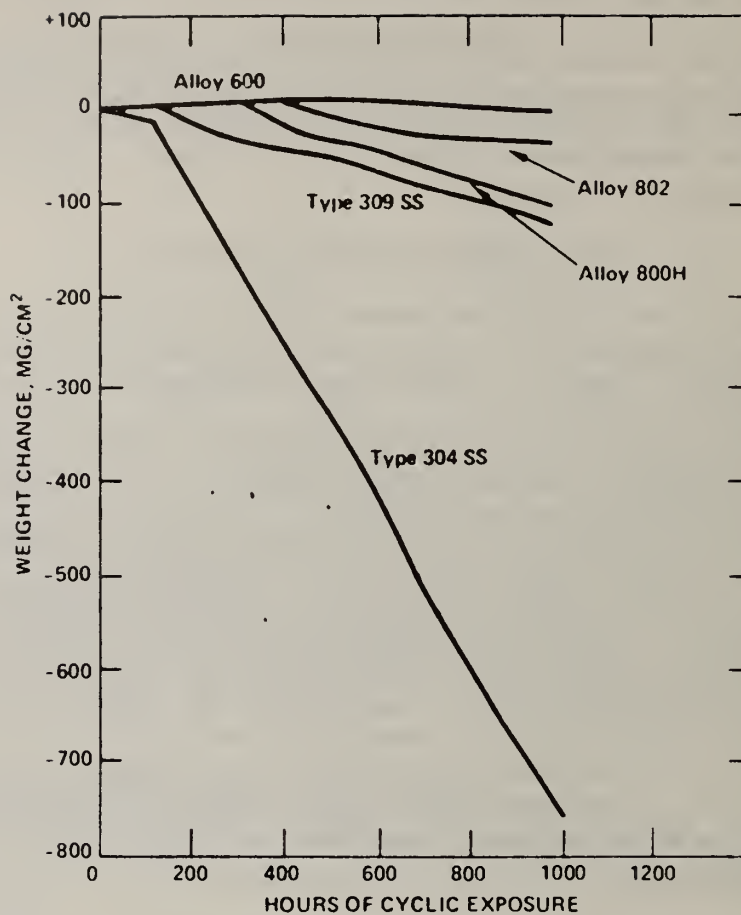


Fig. 1—Scaling resistance at 980°C, of some nickel-iron-chromium alloys. Each cycle consisted of 15 min. exposure to temperature and 5 min. cooling in air.

Note: the performance of alloy 800 itself virtually coincides with 800H under these conditions and alloy 801 is only slightly better than 802 (compare with Fig. 21 in Ref. 2).

Maximum allowable stress, Ksi

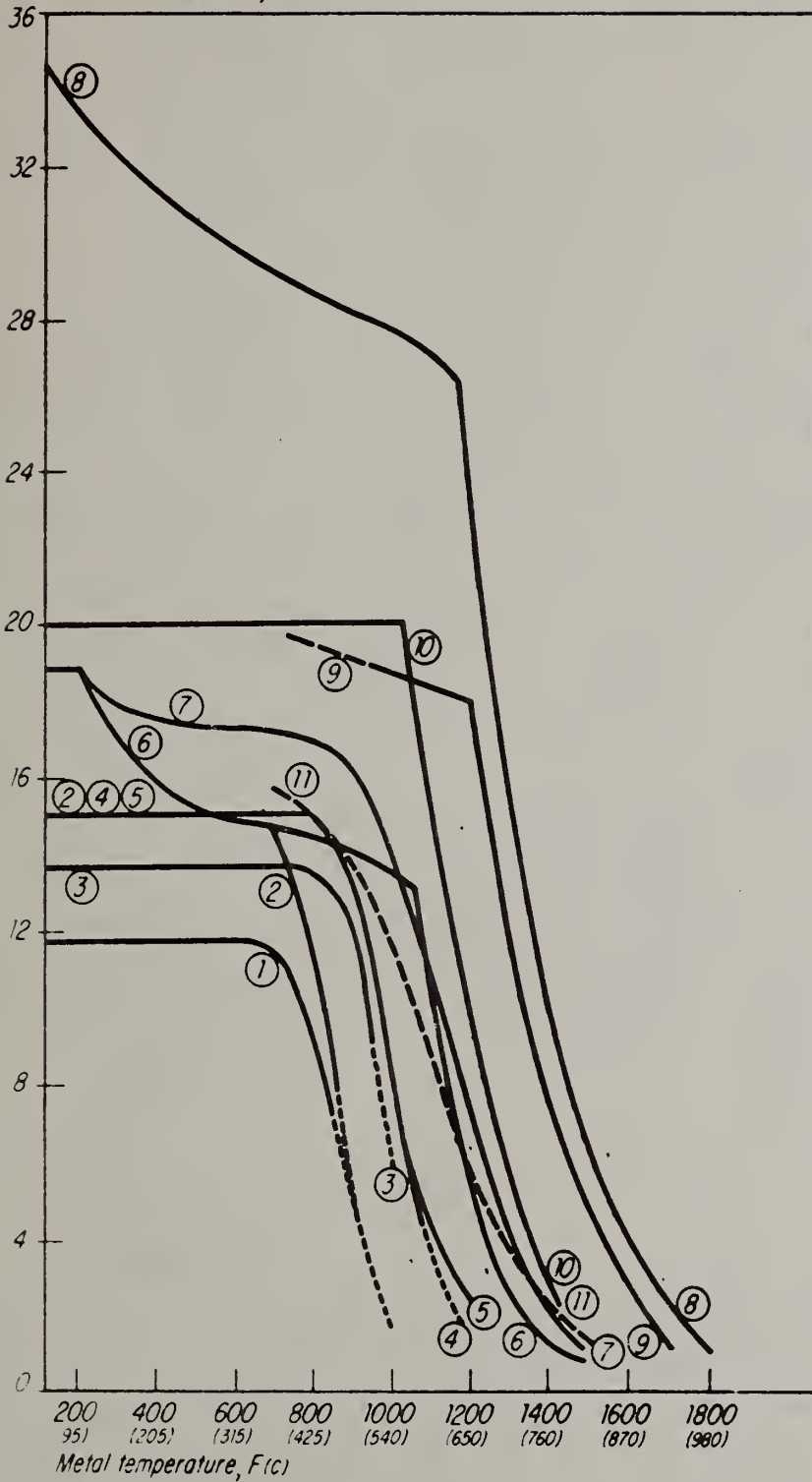


Fig. 2—Estimated relative mechanical strength (in terms of temperature) for candidate heat exchanger materials based on ASME Boiler Code (Criteria for Design Allowable Stresses). (General Electric Co.)

- 1*Carbon steel
 - 2*Carbon steel
 - 3 C-O.5Mo
 - 4 1.25Cr-0.5Mo
 - 5 2.25Cr-1Mo
 - 6 18Cr-10Ni-Ti
 - 7 16Cr-13Ni-3Mo
 - 8 Haynes alloy 188
 - 9 Inconel 617
54Ni-22Cr-12.5Co
-9Mo-1Al
 - 10 Incoloy 800
46Fe-32Ni-20.5Cr
 - 11 AISI type 304
stainless steel
- * Not applicable for advanced steam cycles.

Task M. INFORMATION AND DATA ON MATERIALS FOR MHD-POWER SYSTEMS

1) Data Center for MHD Materials Properties and Performance
(H.M. Ondik, A. Perloff and J.R. Cuthill)

Progress: Regular operations of the Center have continued with regard to handling and cataloguing of contractors' reports.

After investigating a number of possible structure designs for the data base, one version has been deemed most suitable by the Center staff with the concurrence of an expert knowledgeable with respect to the Data Base Management System (DBMS) most likely to be used. This version has been successfully loaded into a computer and will be subjected to detailed testing with real data. It is to be expected that the structure will be modified and evolve as the testing proceeds.

The material required to put out a bid to obtain computer vendors service has been prepared with full specifications and has been delivered to the Department of Commerce. The Department rules do not permit the specification of a specific DBMS and, with the wide choice of vendors available, it is possible that we may not end up with the DBMS for which our data base structure was designed. However, any system meeting our specifications should be able to accept our data structure with relatively minor modifications. Therefore, any such problems should cause only minor delays, if any.

Additional equipment for the computer-terminal facility, a hard copy unit and two terminal stands, have been received. There have been delays in getting the promised room and necessary telephone lines for our facility due to the non-availability of workmen arising from reorganization-caused reconstruction around the Bureau. We are still hopeful of getting our facility done in the near future. In the meantime testing will proceed using other available facilities.

A meeting of University of Tennessee Space Institute personnel and NBS personnel took place this quarter to discuss possible cooperative projects. We used this opportunity to present the Data Center plans and progress to them and to get helpful feedback from them on user needs and desires.

Plans: The regular operations of the center, i.e. review and cataloguing of contractors' reports and extraction of data from them, will continue. Additional contact with the user community is anticipated to get additional useful feedback. Data base structure modifications and testing should accelerate.